

APPENDIX 1. NSAIDs BASED ROMP NANOPARTICLES: SYNTHESIS, SELF-ASSEMBLY AND DRUG RELEASE.

1. NMR spectra

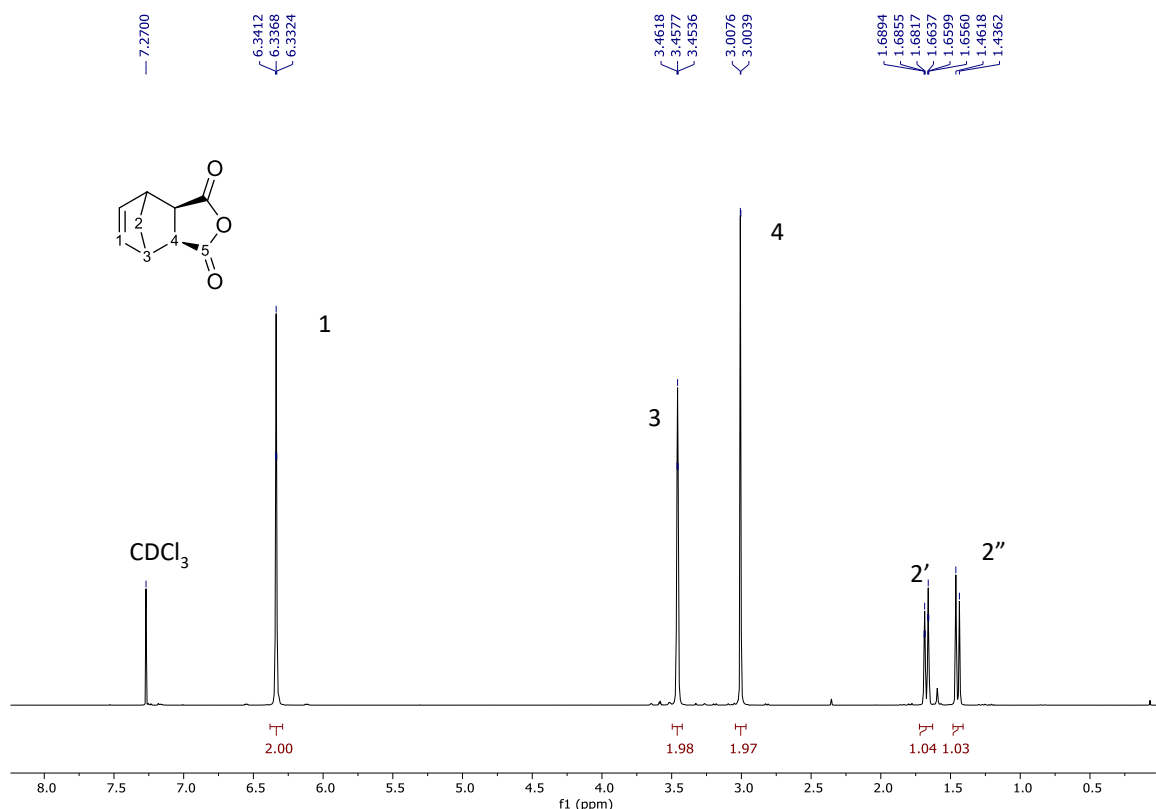


Fig. S1. ^1H NMR in CDCl_3 of *exo*-carbic anhydride, **1b**

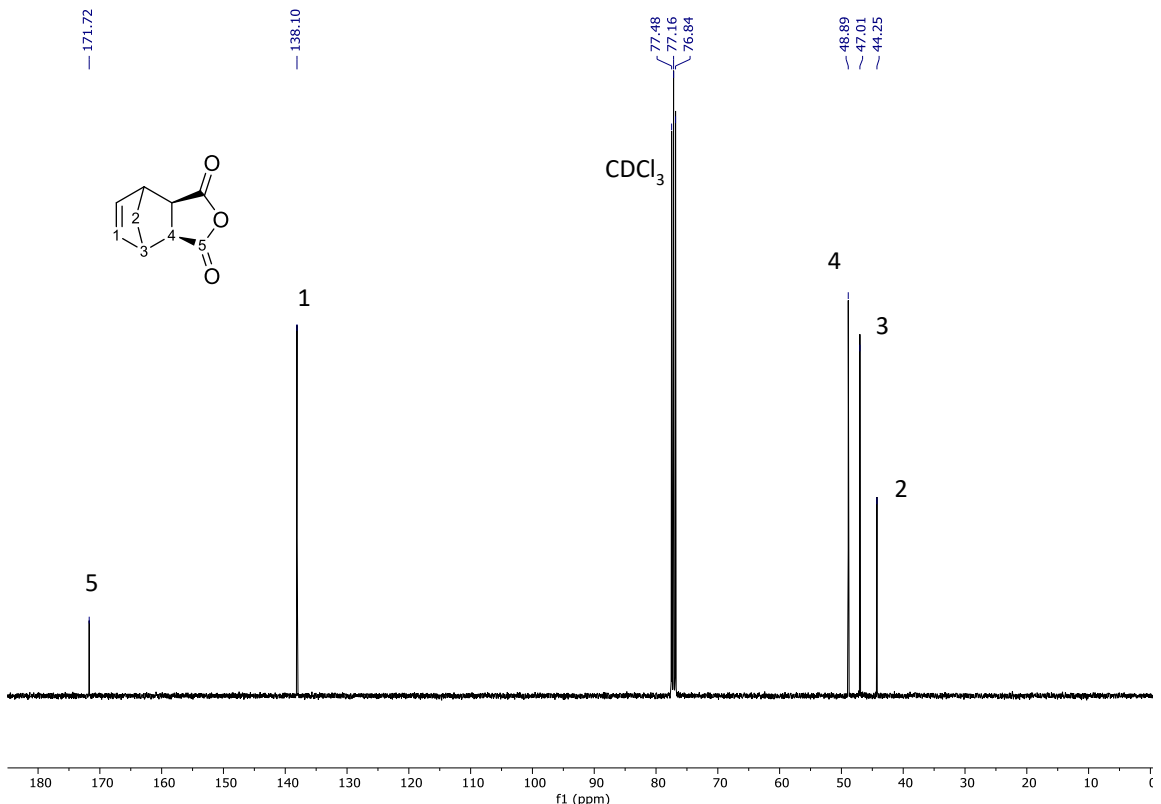


Fig. S2. ^{13}C NMR in CDCl_3 of *exo*-carbic anhydride, **1b**

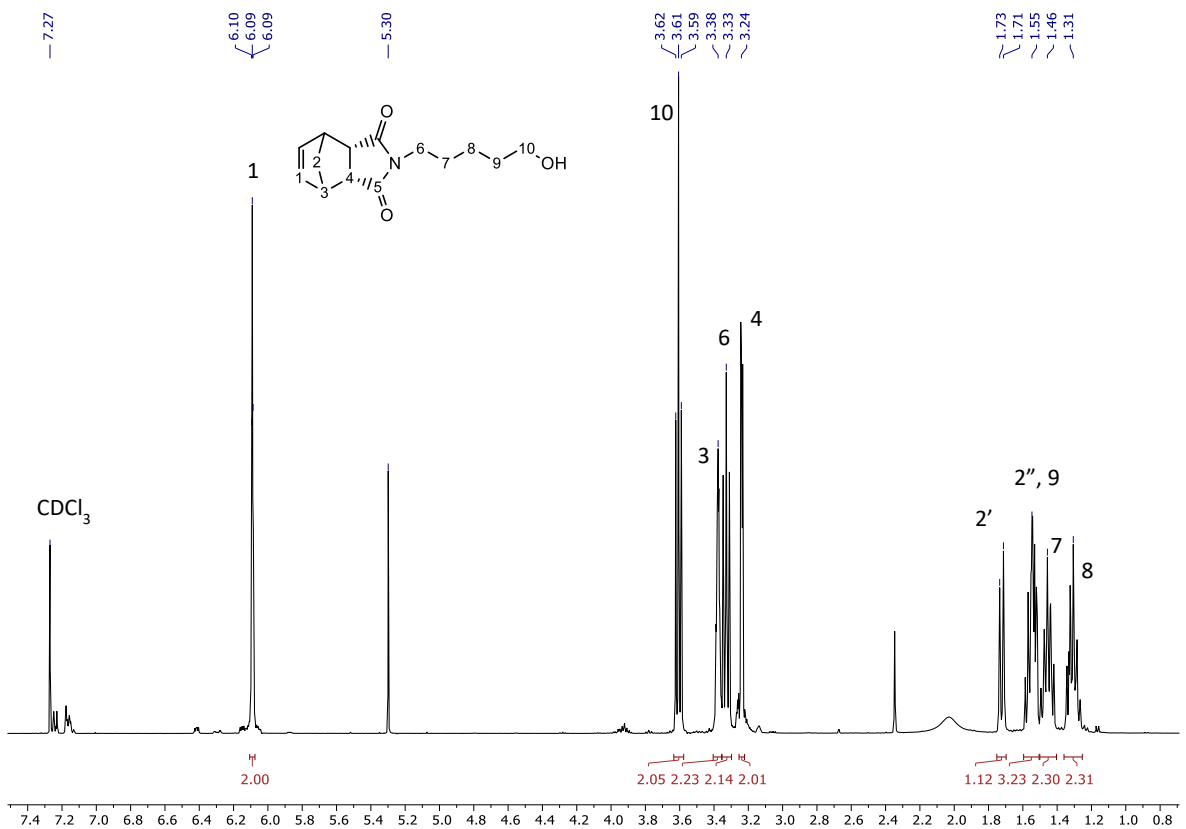


Fig. S3. ^1H NMR in CDCl_3 of *N*-(hydroxypentanyl)-*cis*-5-norbornene-*endo*-2,3-dicarboximide, **3a**

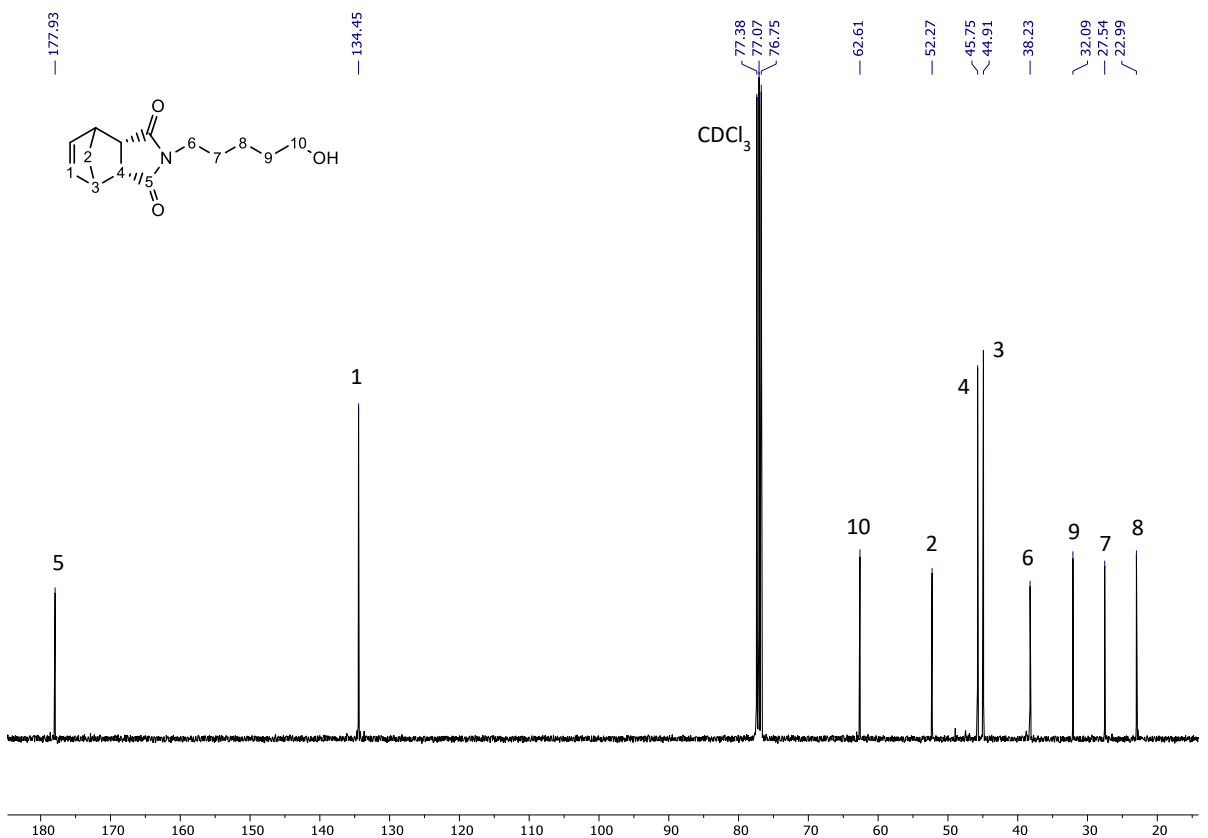


Fig. S4. ¹³C NMR in CDCl₃ of *N*-(hydroxypentanyl)-*cis*-5-norbornene-*endo*-2,3-dicarboximide, **3a**

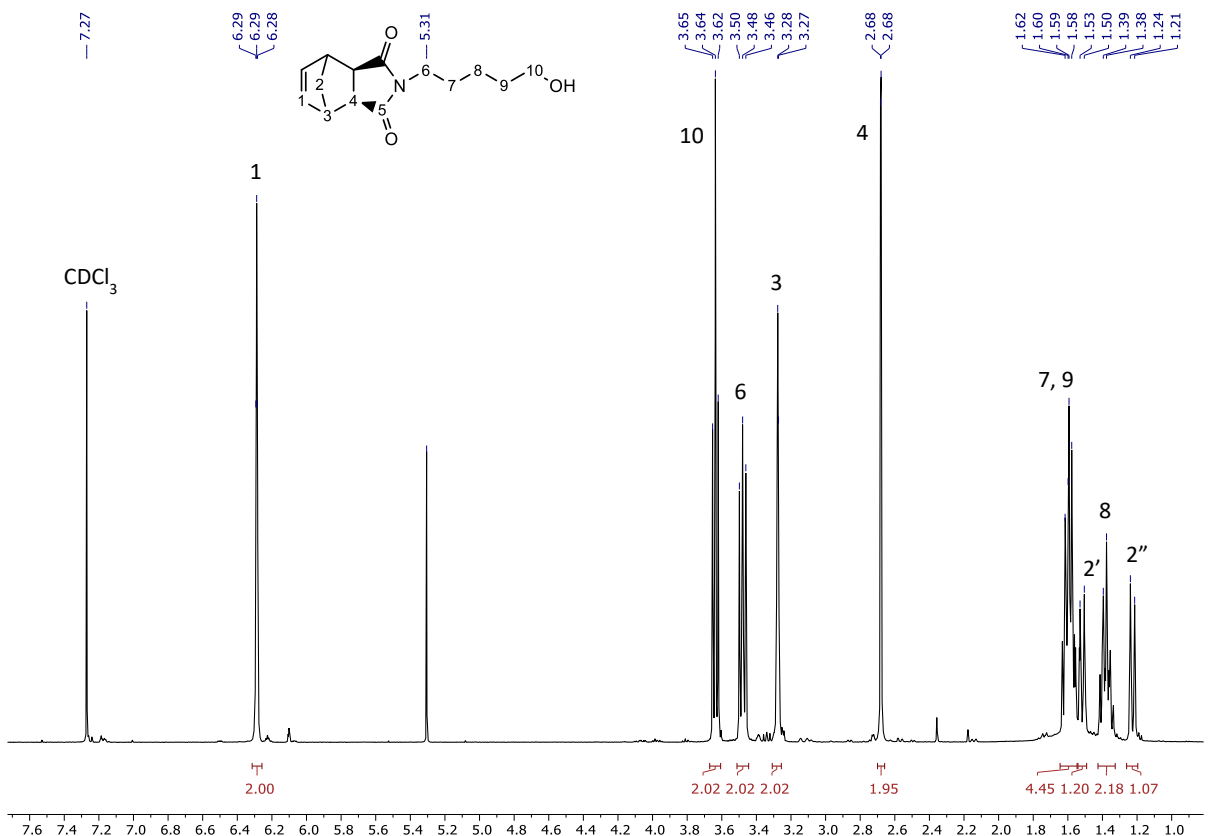


Fig. S5. ¹H NMR in CDCl₃ of *N*-(hydroxypentanyl)-*cis*-5-norbornene-*exo*-2,3-dicarboximide **3b**

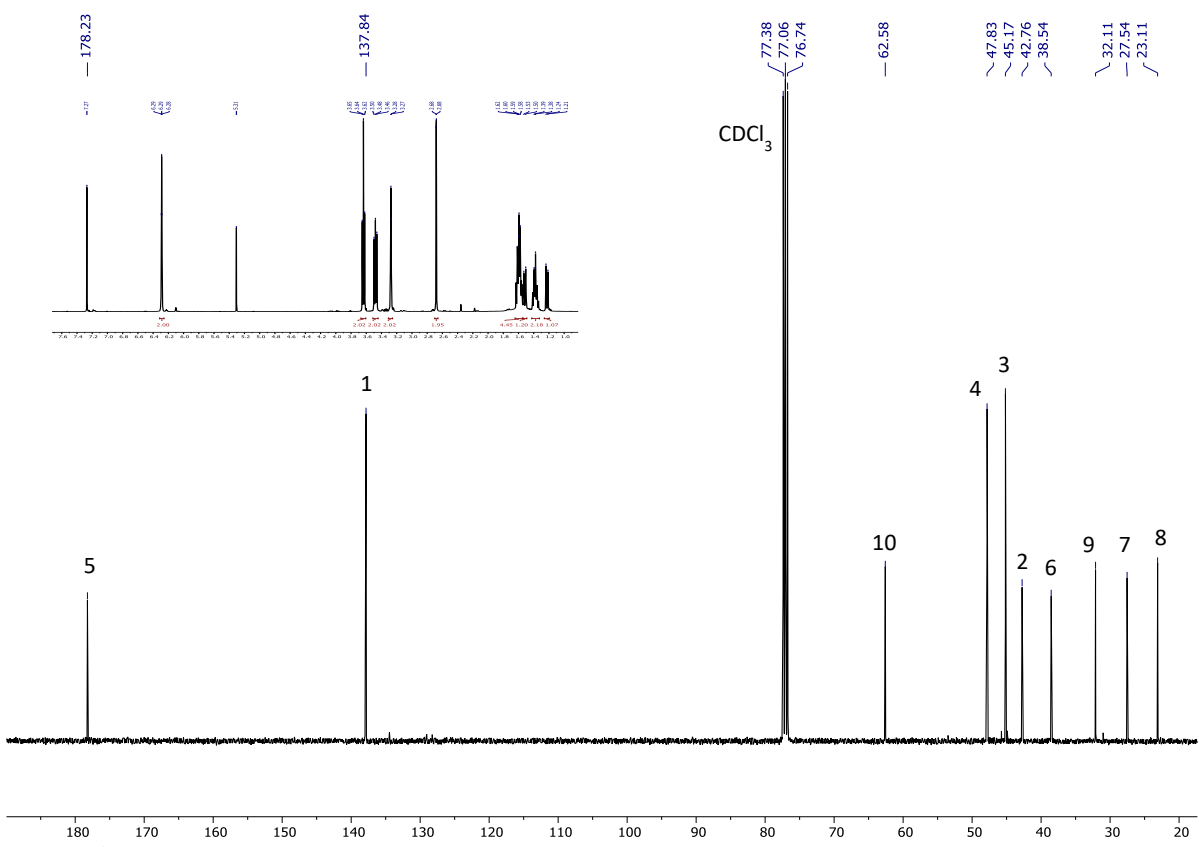


Fig. S6. ^{13}C NMR in CDCl_3 of N -(hydroxypentanyl)-*cis*-5-norbornene-*exo*-2,3-dicarboximide **3b**

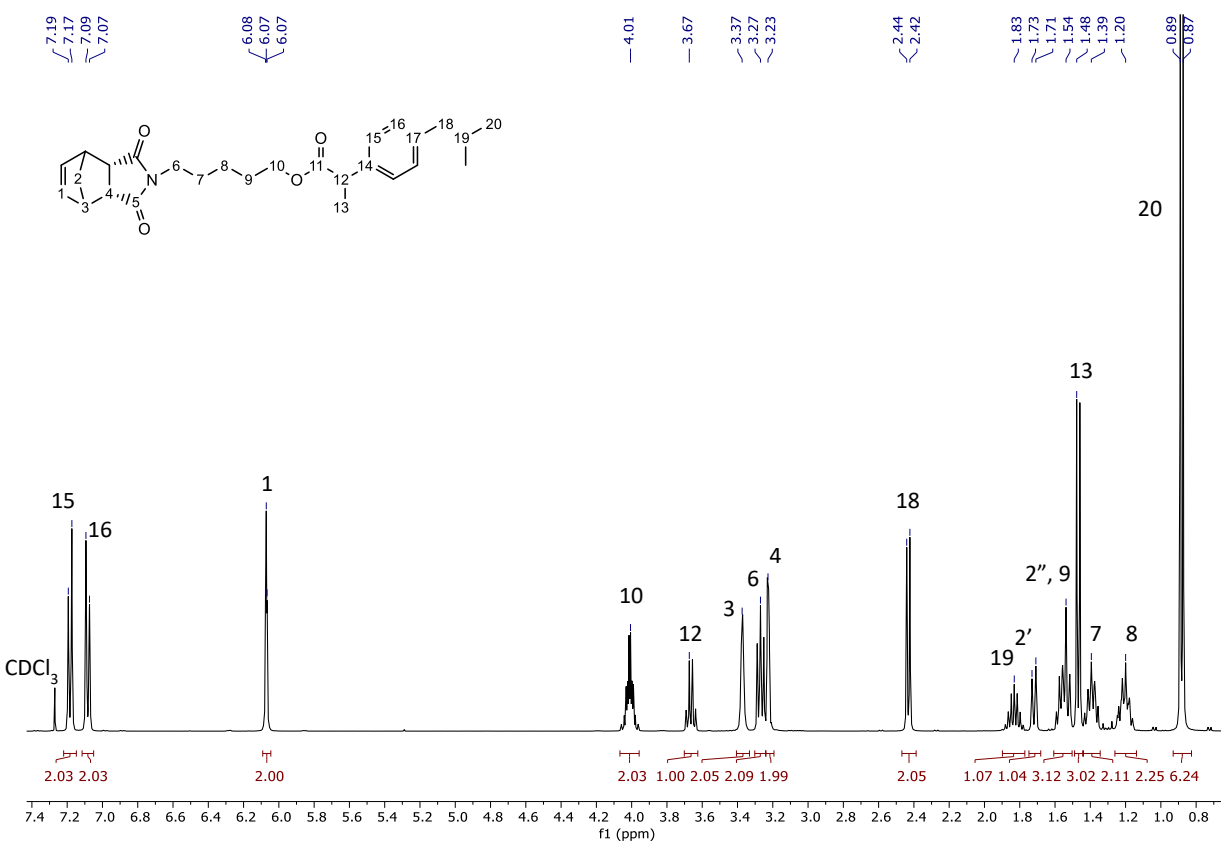


Fig. S7. ^1H NMR in CDCl_3 of ibuprofen ester of compound **3a**, **5a**

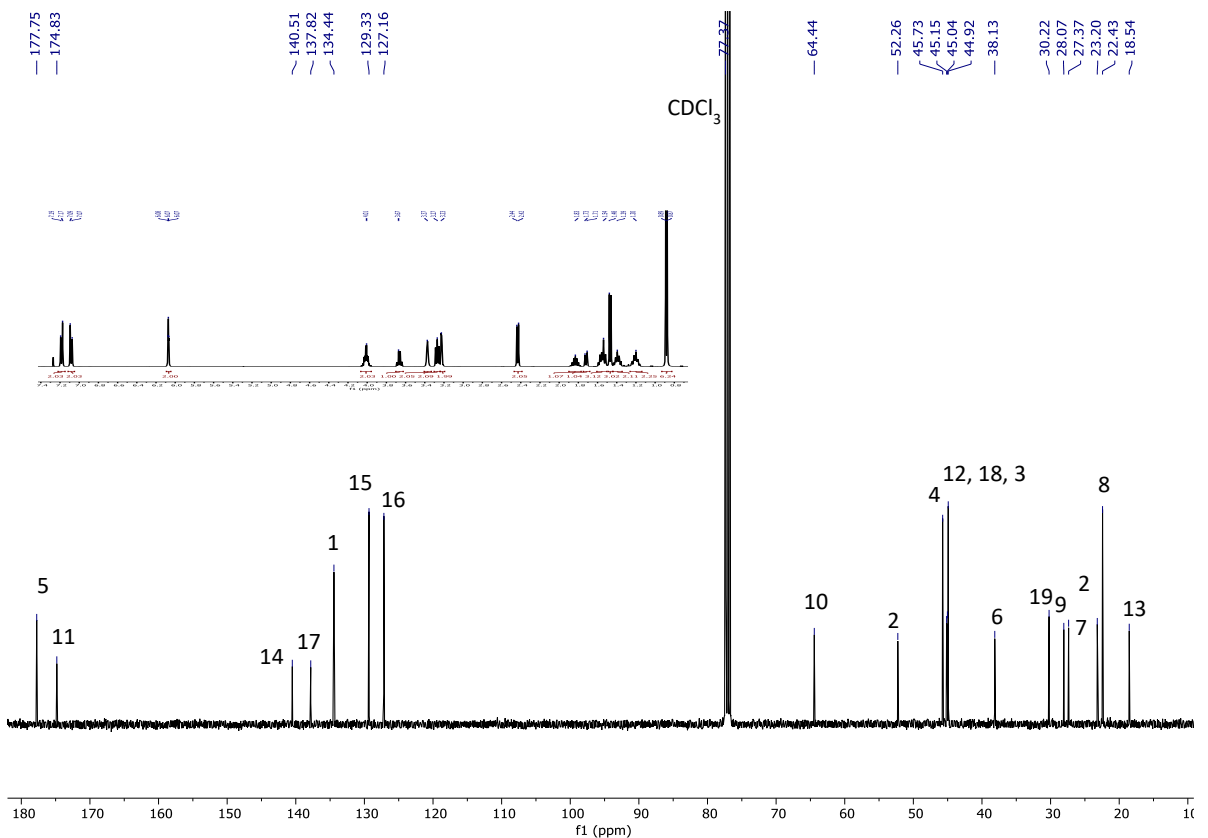


Fig. S8. ^{13}C NMR in CDCl_3 of Ibuprofen ester of compound 3a, **5a**

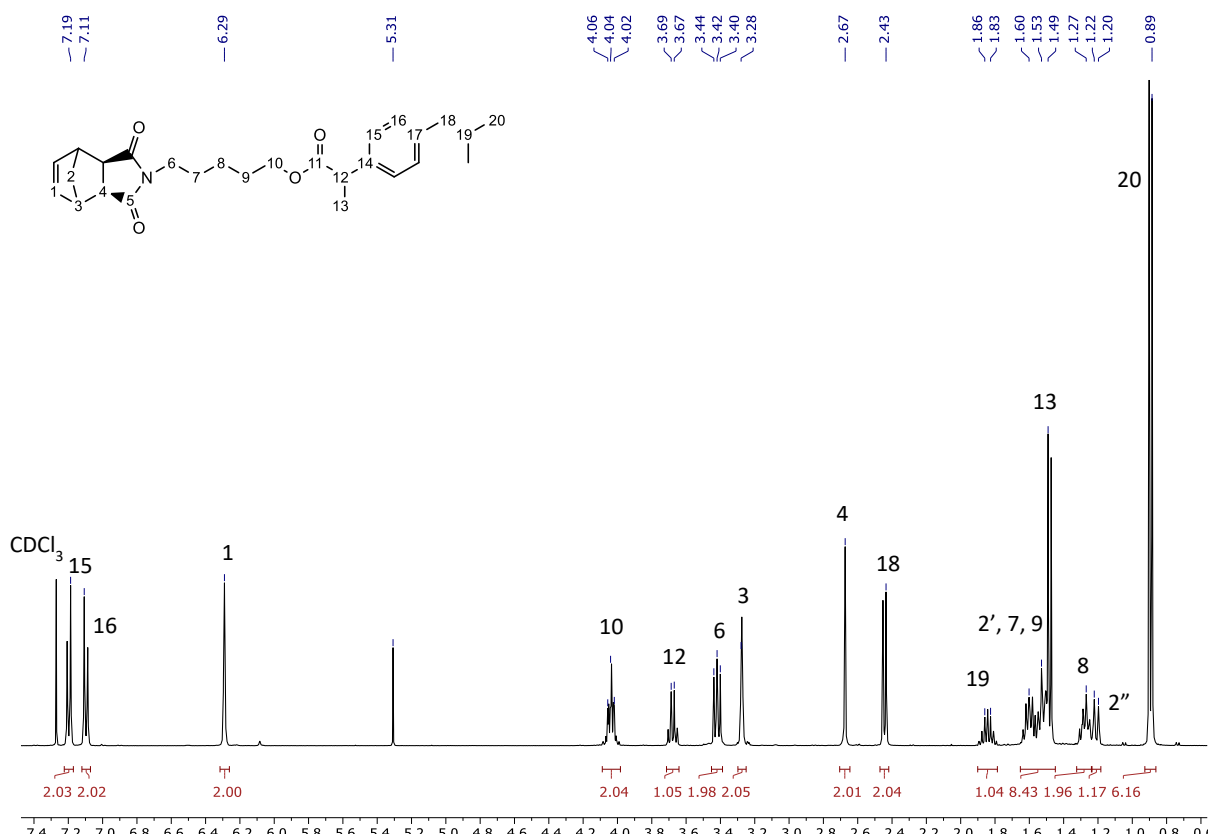


Fig. S9. ^1H NMR in CDCl_3 of Ibuprofen ester of compound 3b, monomer **5b** (NB-Ibu)

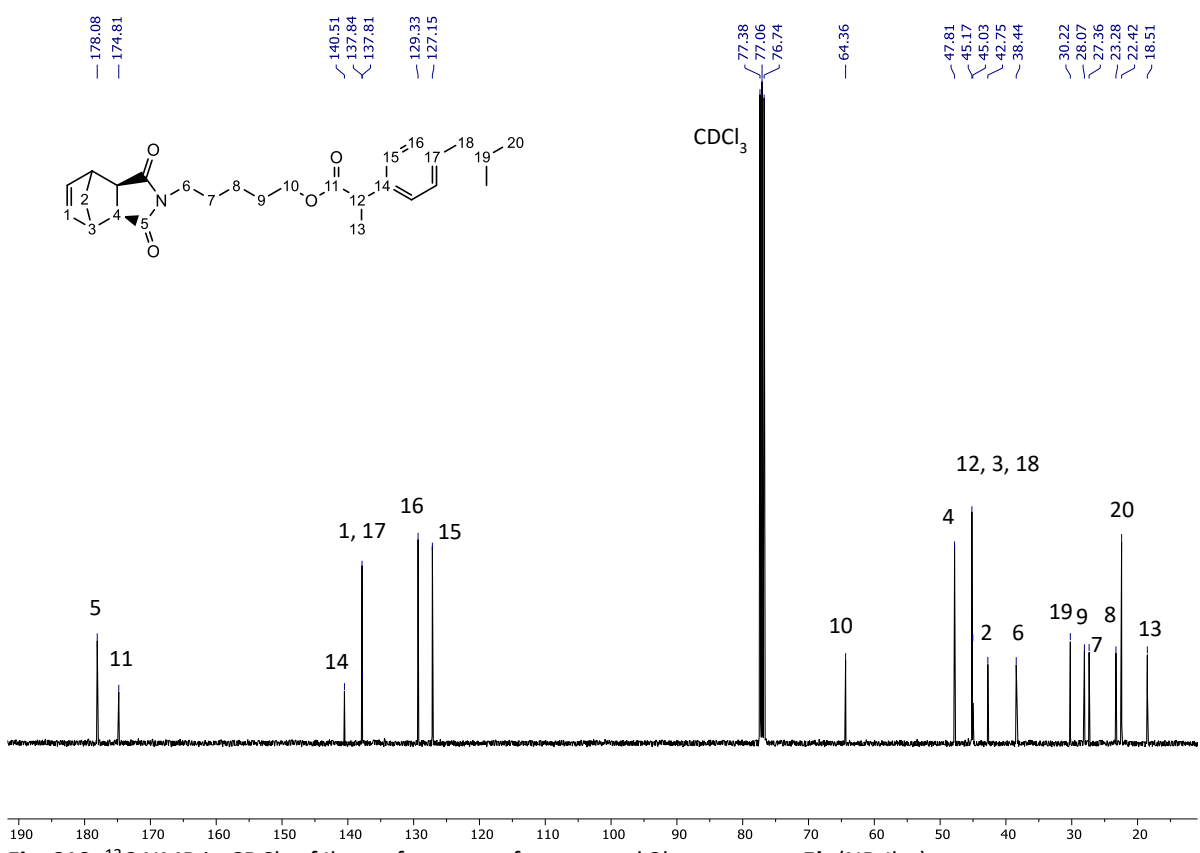


Fig. S10. ^{13}C NMR in CDCl_3 of Ibuprofen ester of compound 3b, monomer **5b** (NB-Ibu)

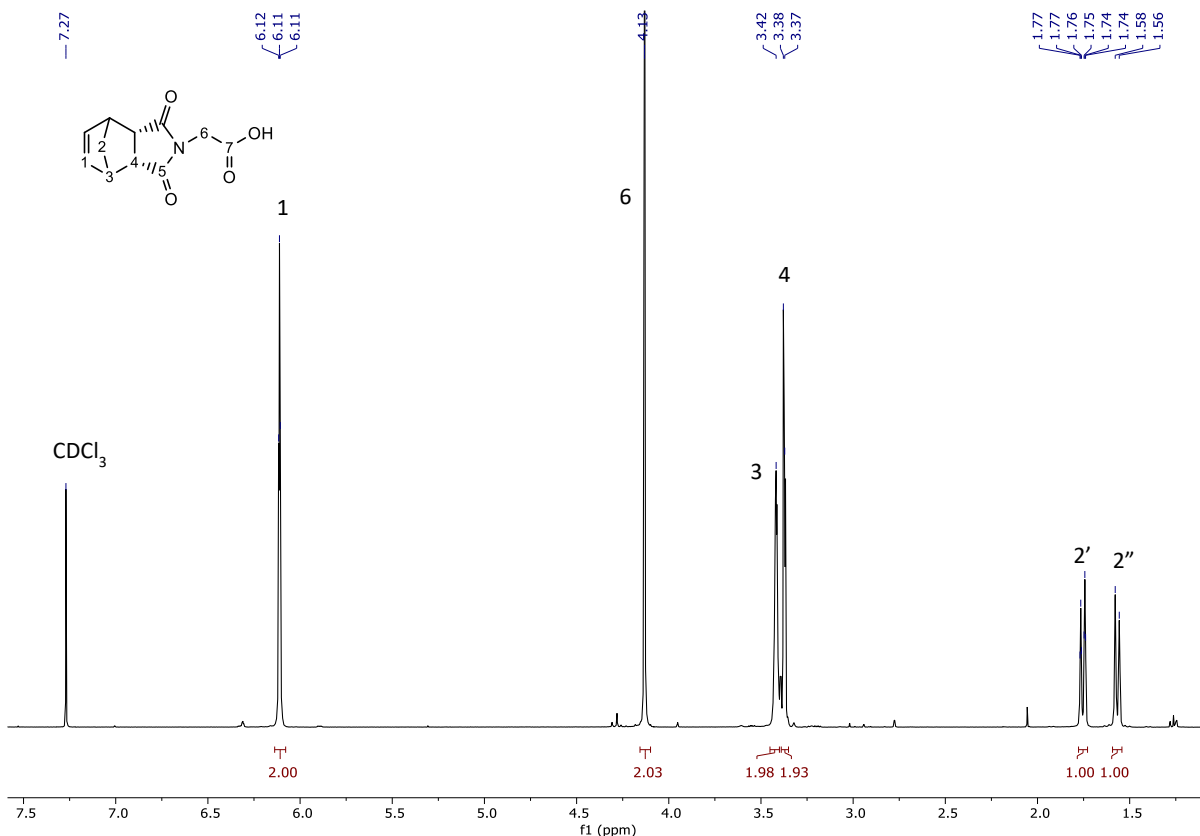


Fig. S11. ^1H NMR in CDCl_3 of *N*-(*endo*-himoyl)-glycine, **7a**

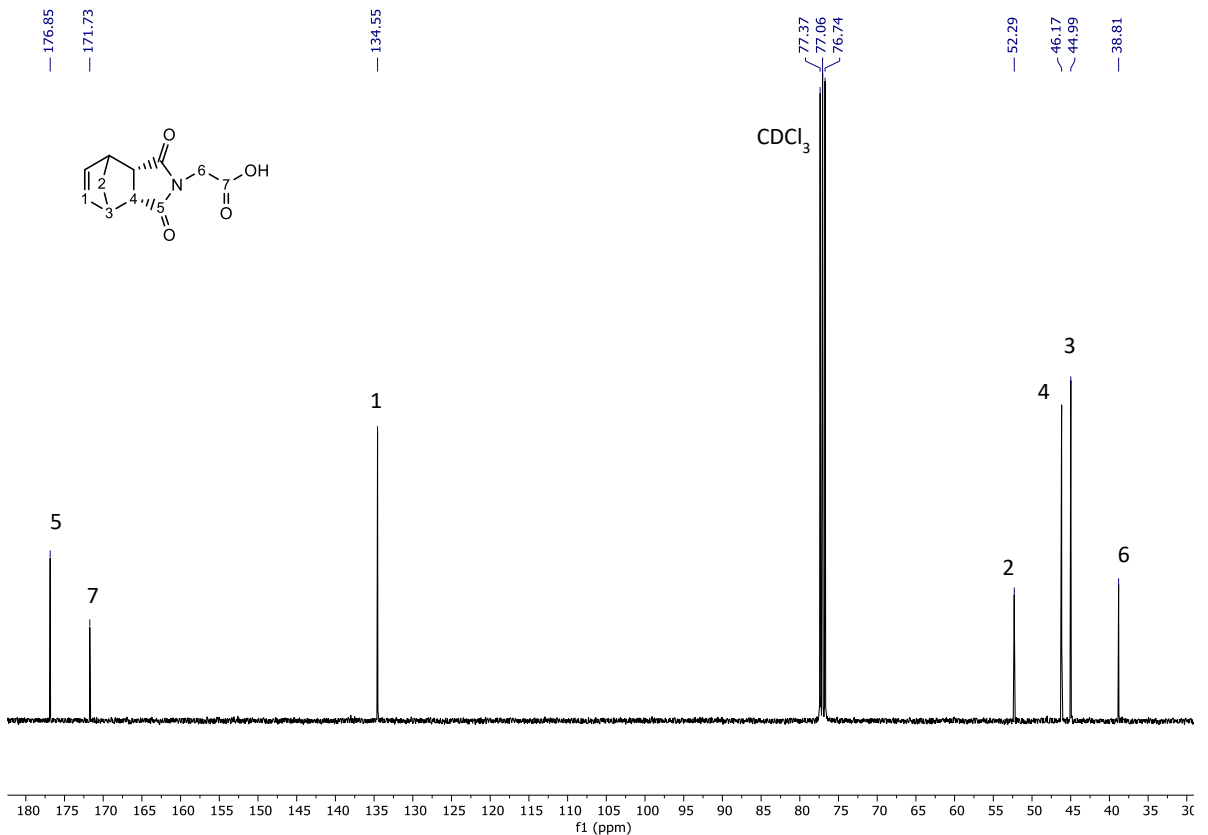


Fig. S12. ¹³C NMR in CDCl₃ of *N*-(*endo*-himoyl)-glycine, **7a**

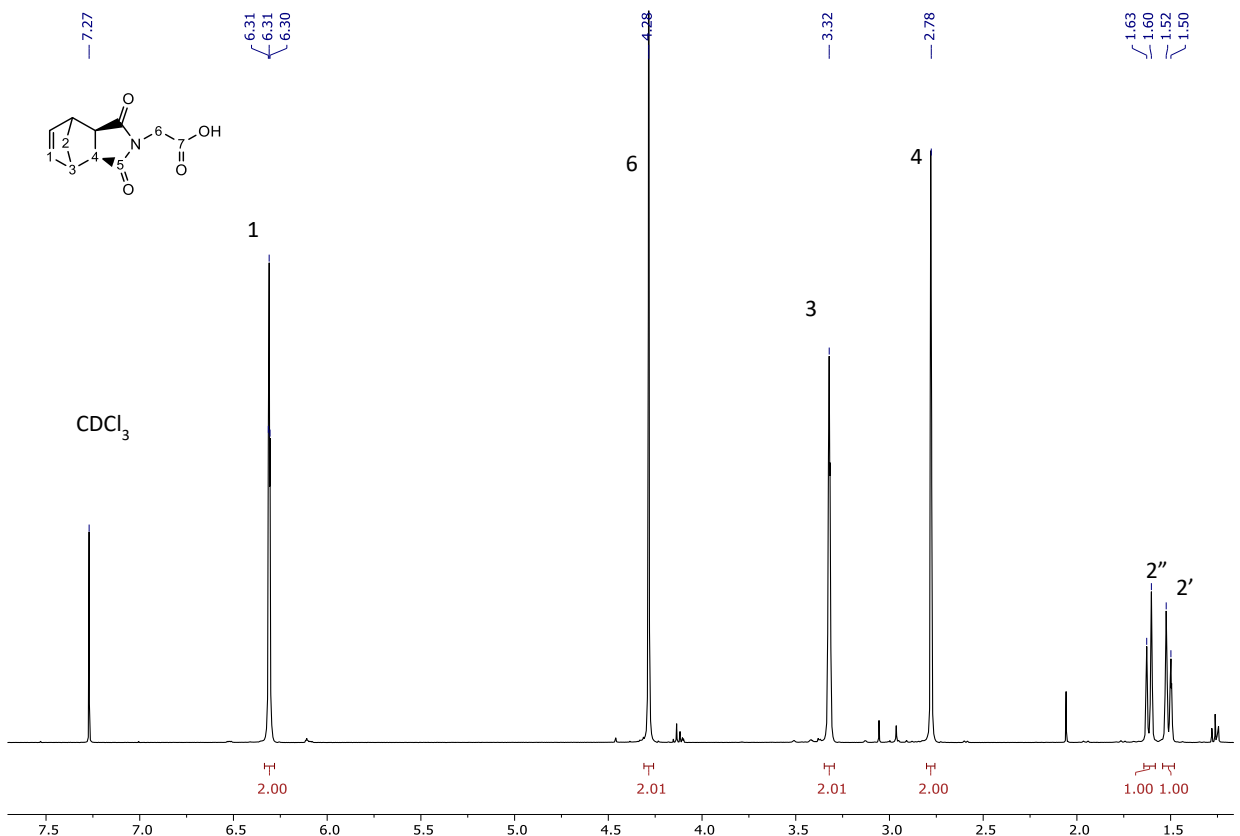


Fig. S13. ¹H NMR in CDCl₃ of *N*-(*exo*-himoyl)-glycine, **7b**

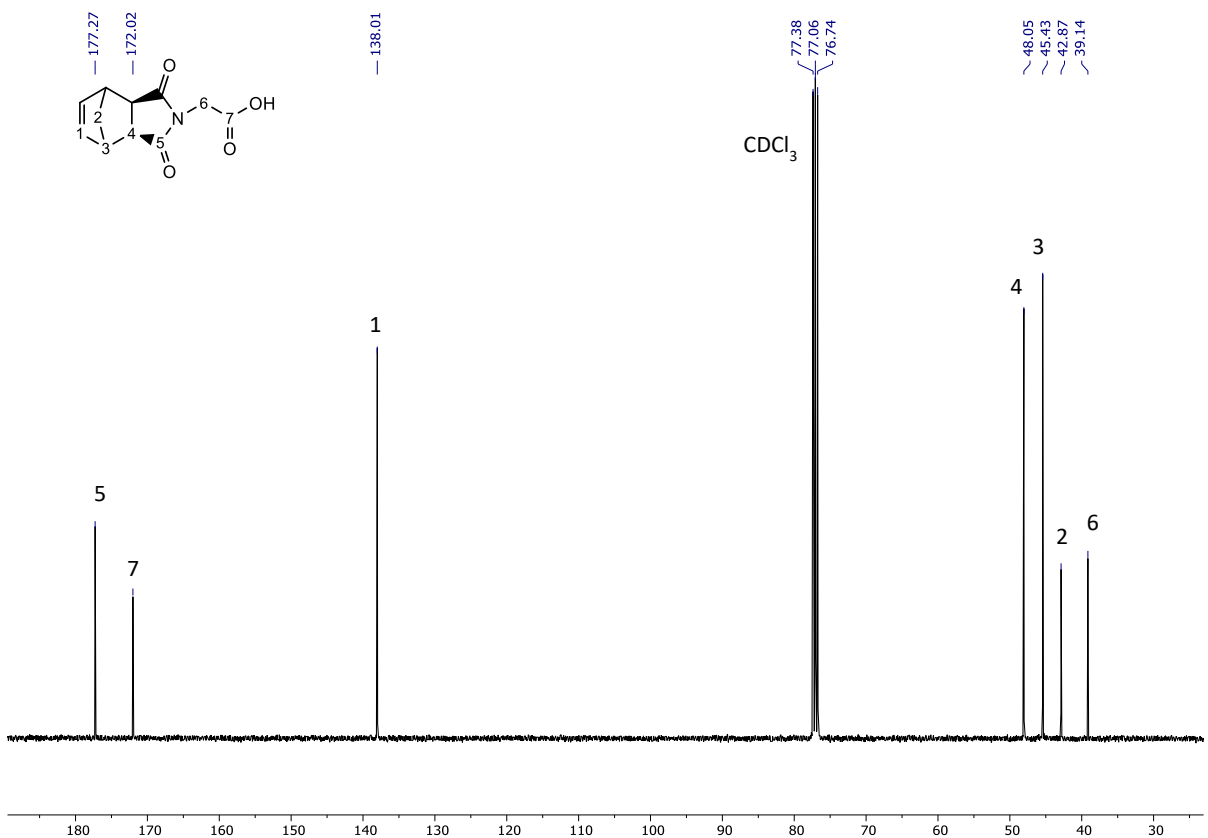


Fig. S14. ^{13}C NMR in CDCl_3 of N -(*exo*-himoyl)-glycine, **7b**

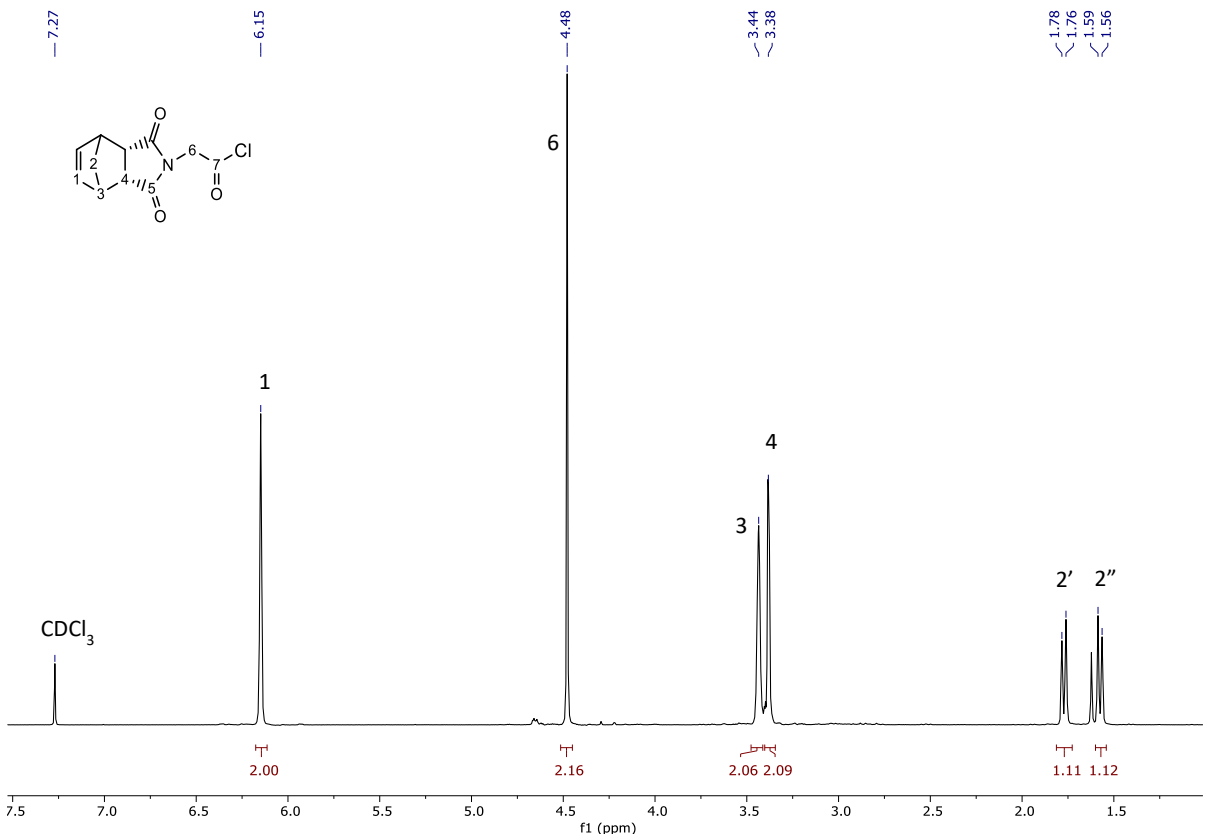
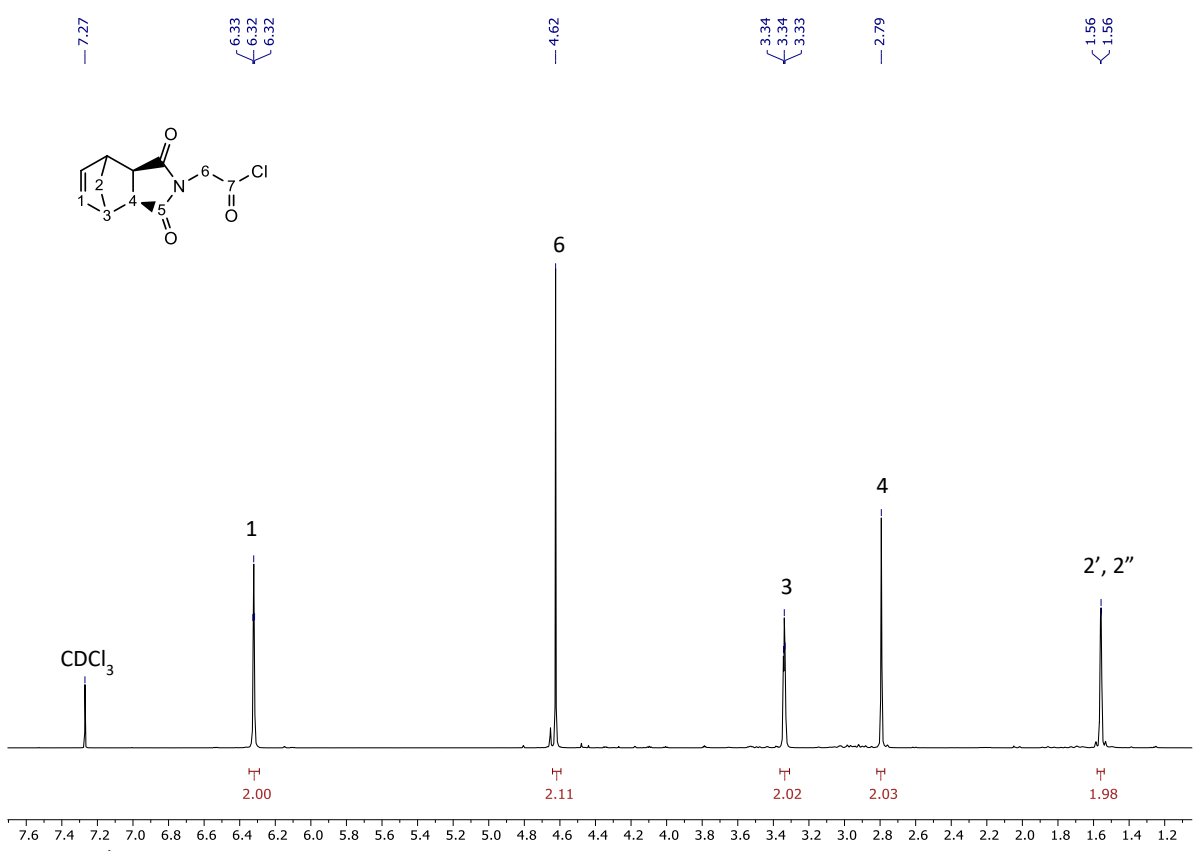
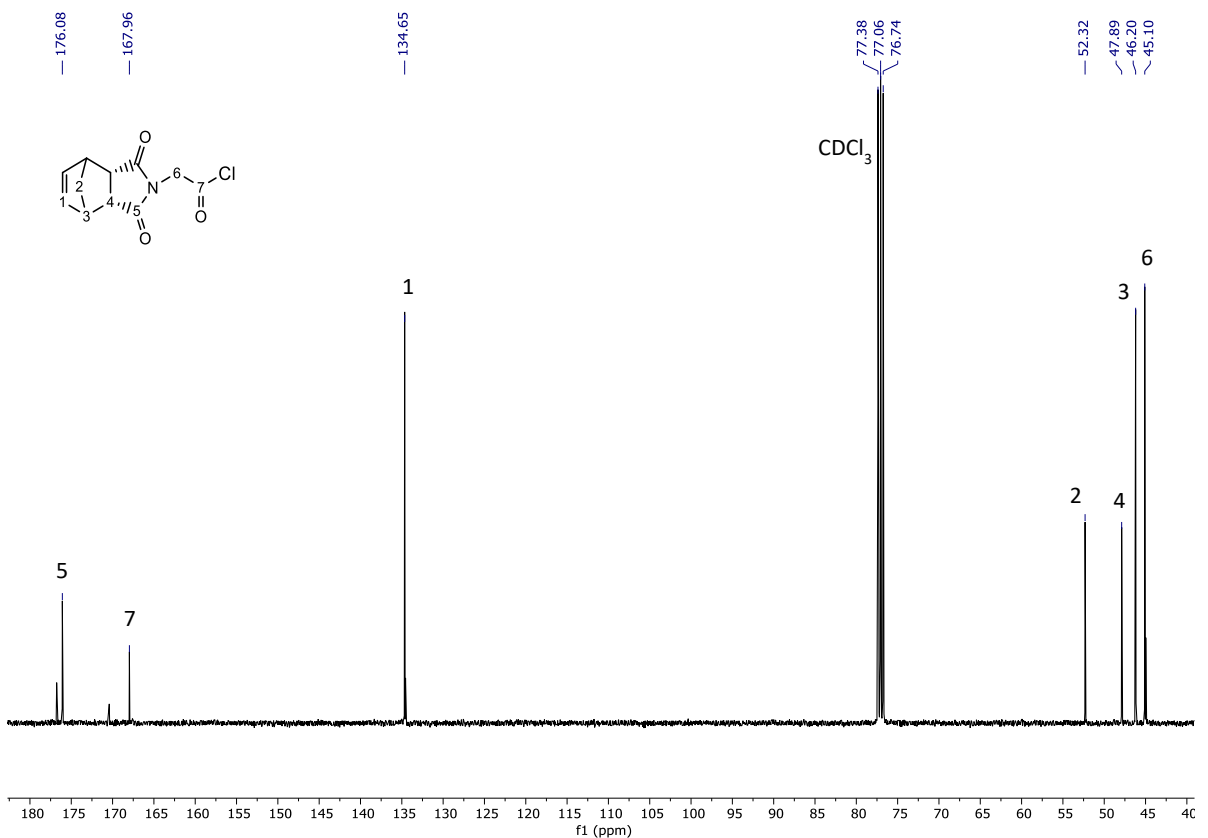


Fig. S15. ^1H NMR in CDCl_3 of N -(*endo*-himoyl)-glycinoyl chloride, **8a**



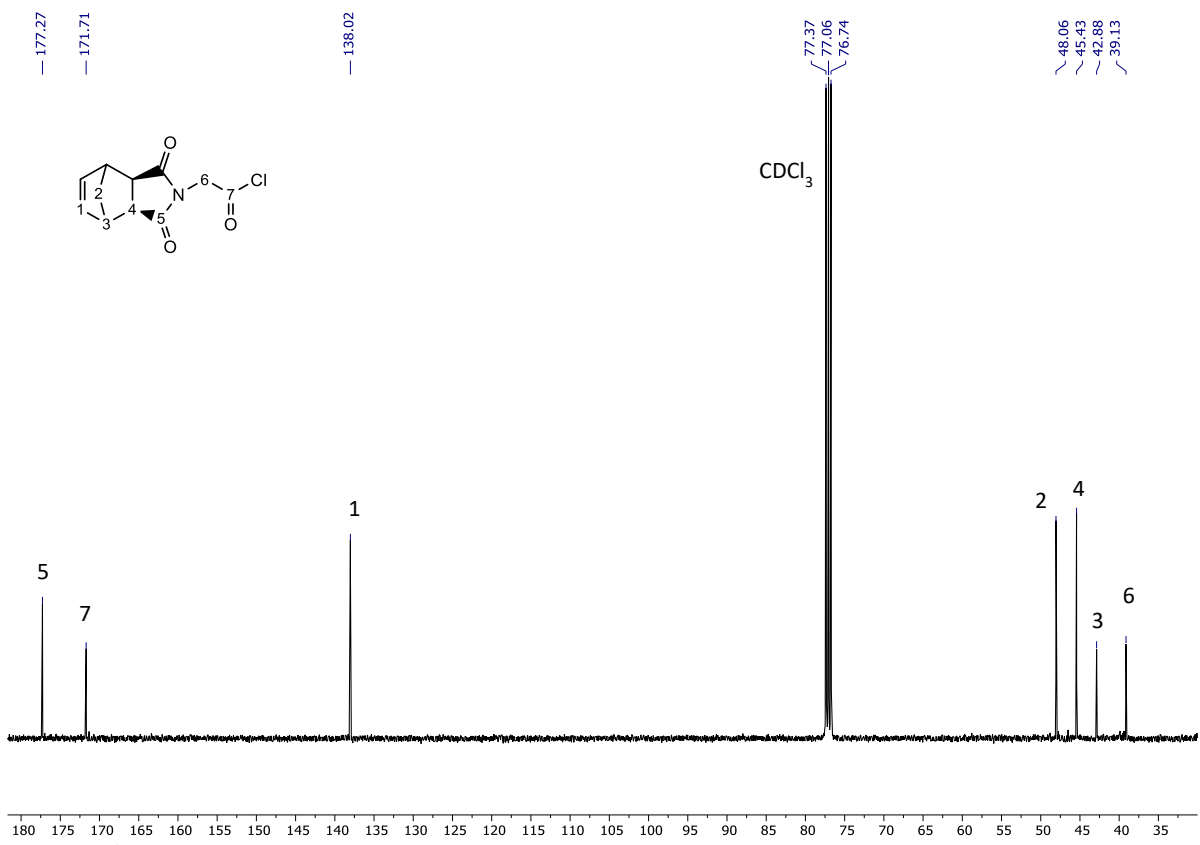


Fig. S18. ¹³C NMR in CDCl₃ of *N*-(*exo*-himoyl)-glycinoyl chloride, **8b**

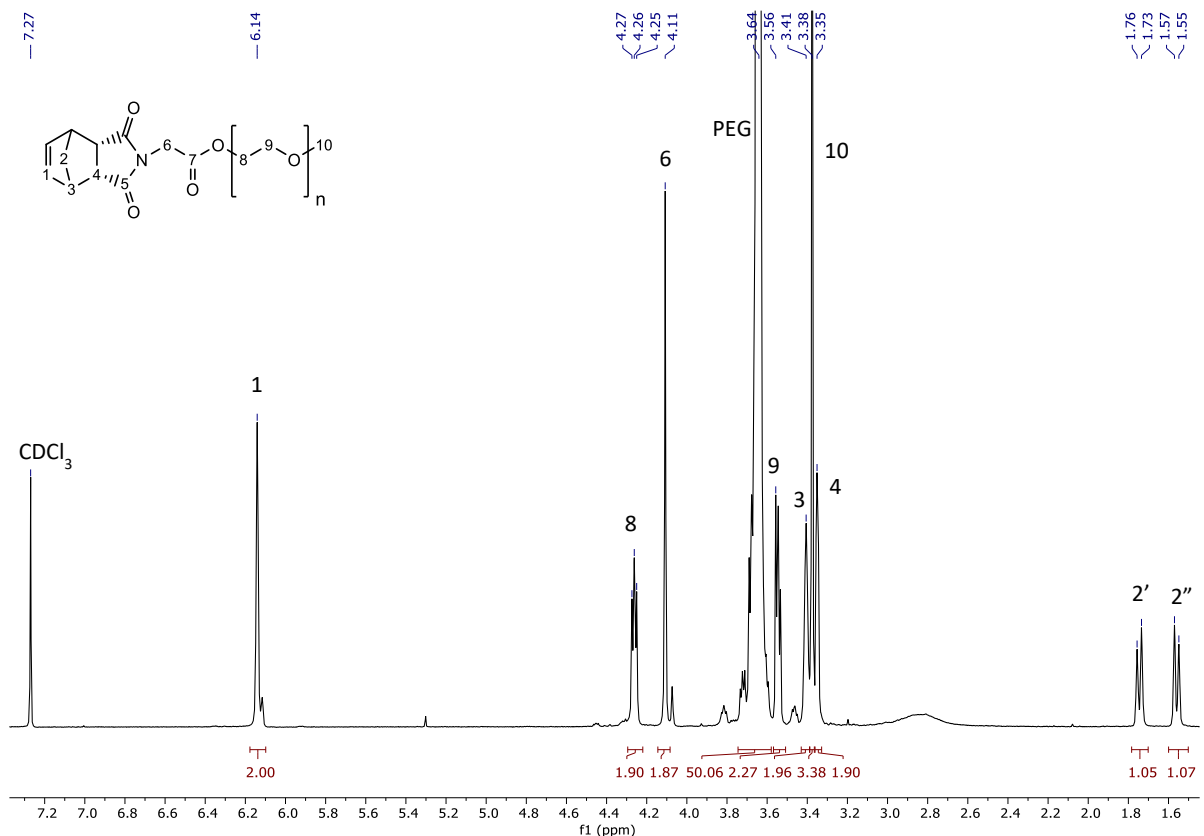


Fig. S19. ¹H NMR in CDCl₃ of *N*-(*endo*-himoyl)-glycine PEG-OMe ester, **10a**

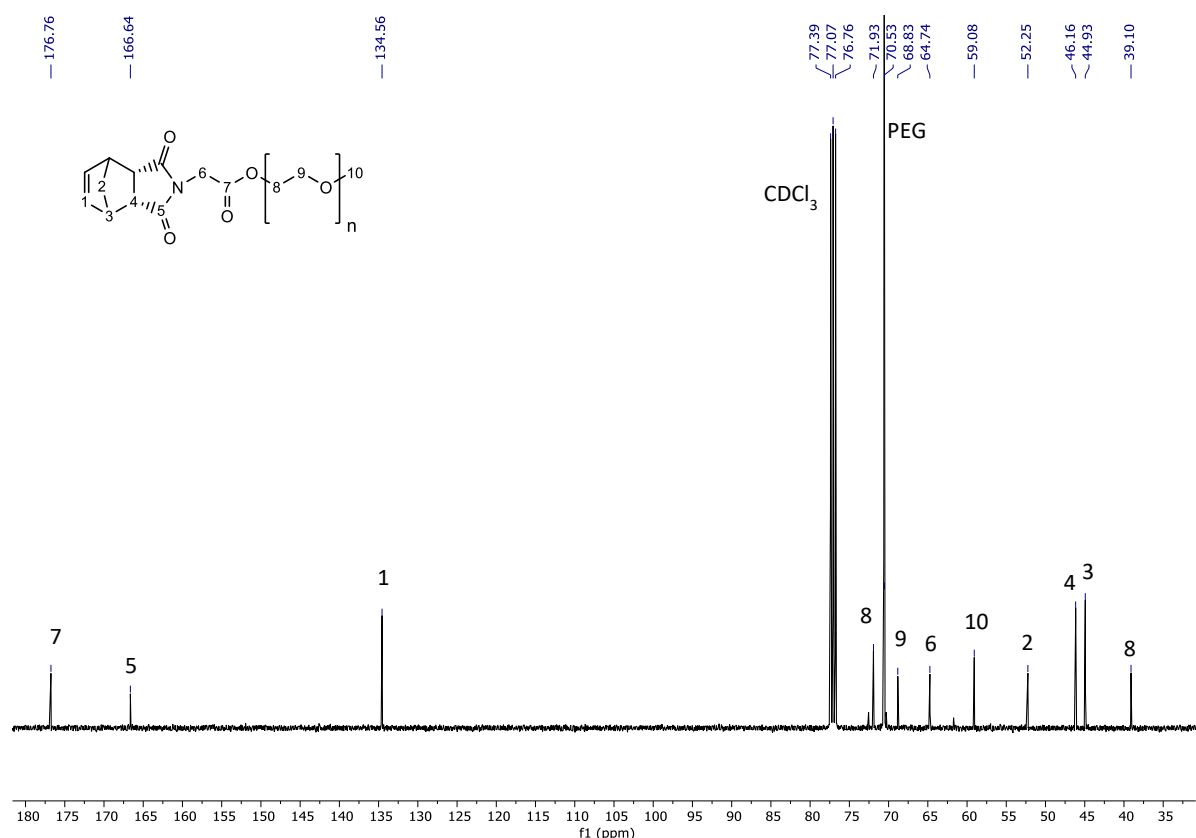


Fig. S20. ^{13}C NMR in CDCl_3 of *N*-(*endo*-himoyl)-glycine PEG-OMe ester, **10a**

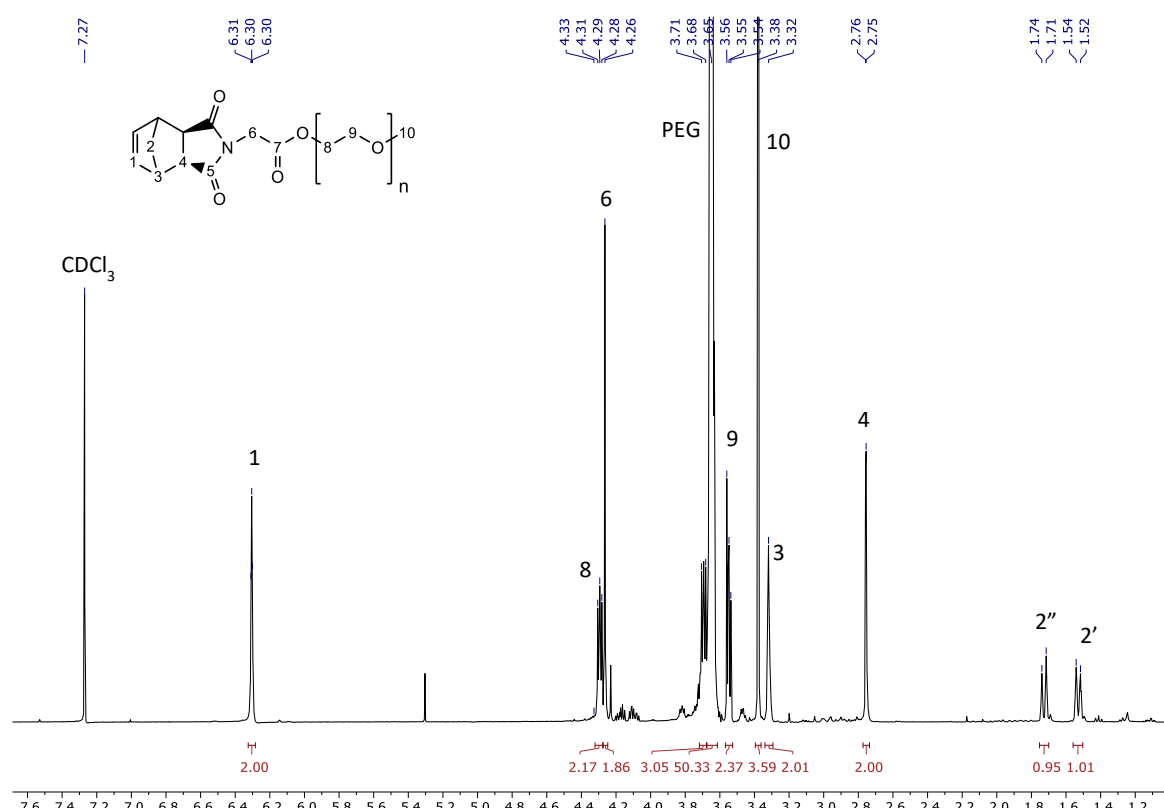


Fig. S21. ^1H NMR in CDCl_3 of *N*-(*exo*-himoyl)-glycine PEG-OMe ester, monomer **10b** (NB-PEG)

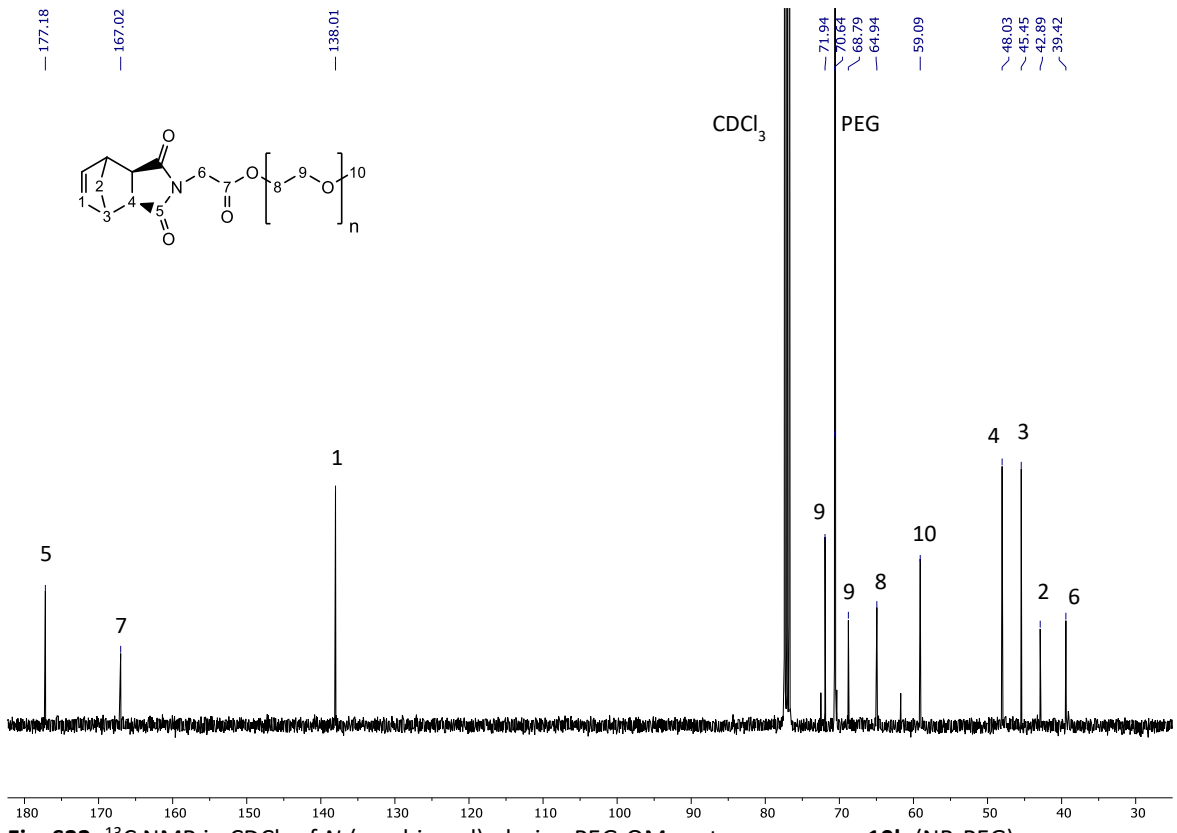


Fig. S22. ^{13}C NMR in CDCl_3 of *N*-(*exo*-himoyl)-glycine PEG-OMe ester, monomer **10b** (NB-PEG)

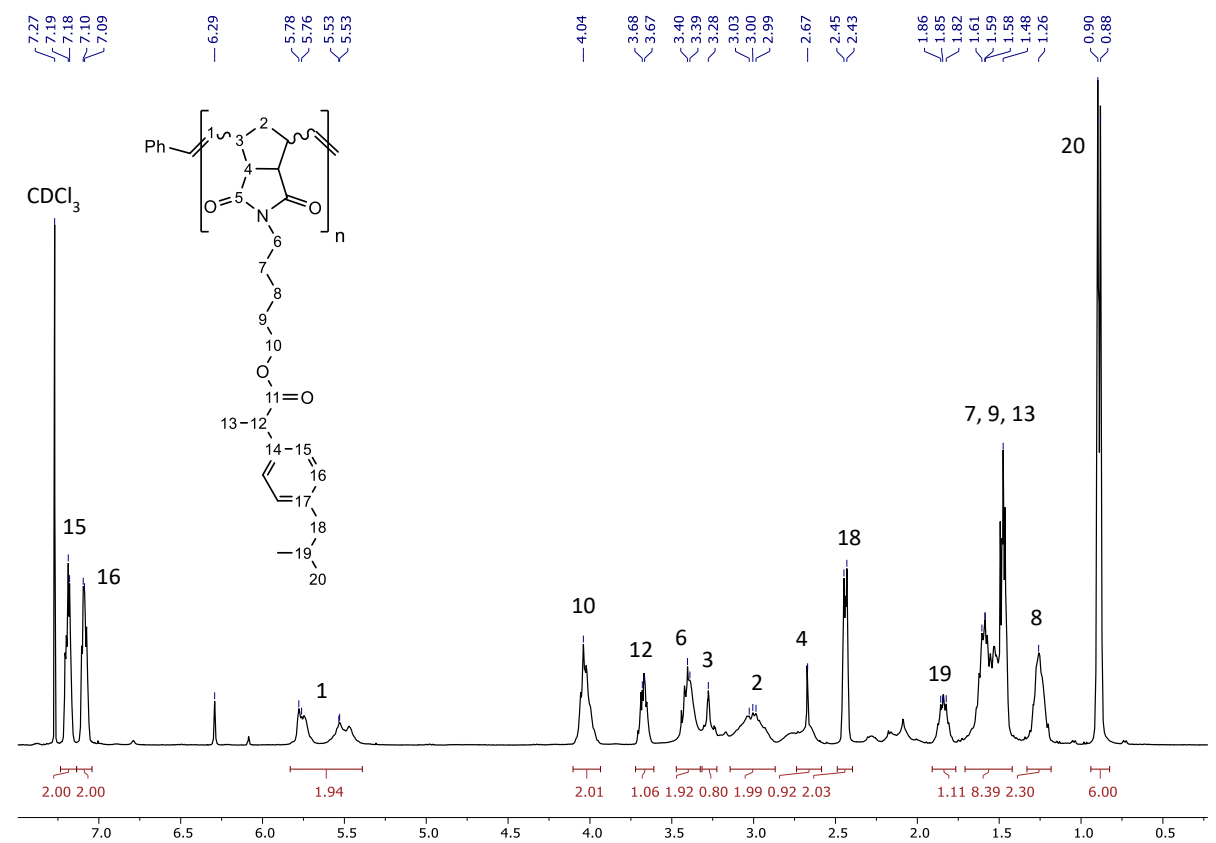
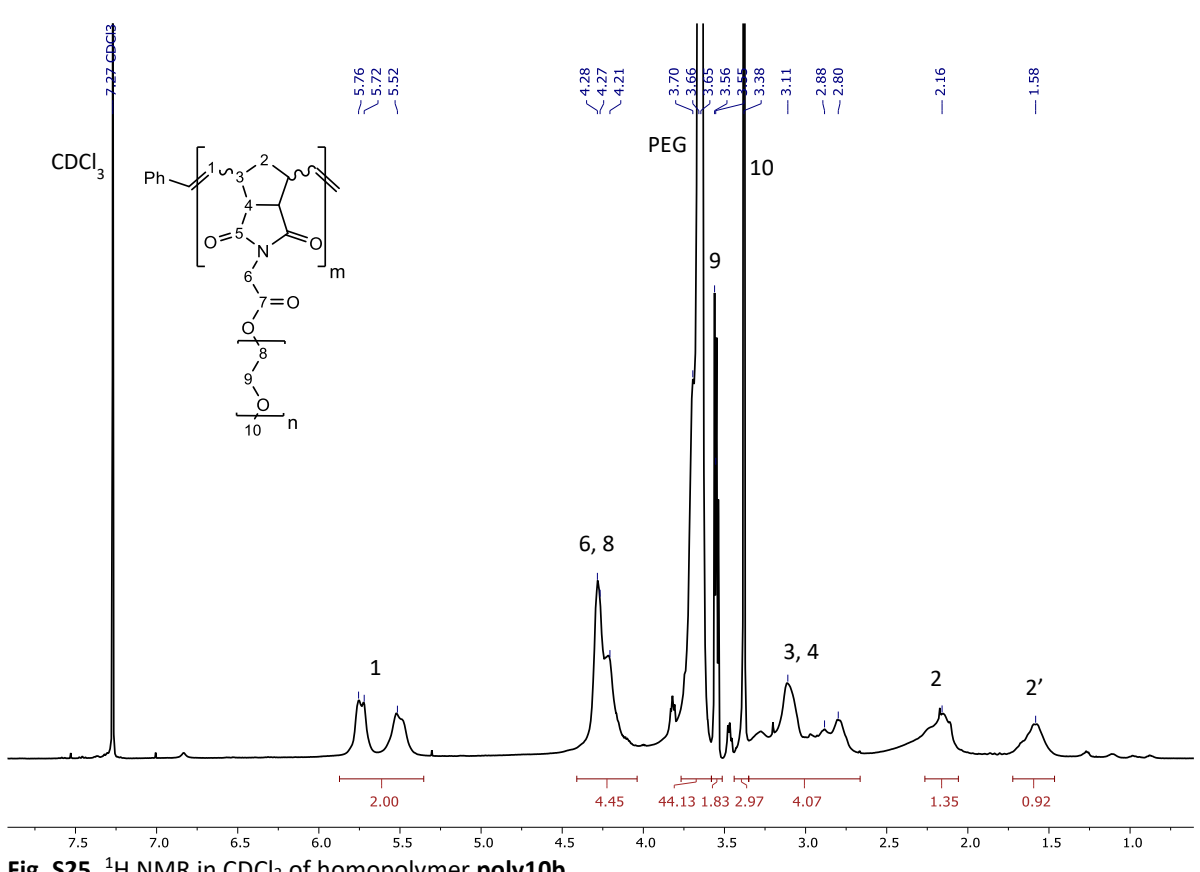
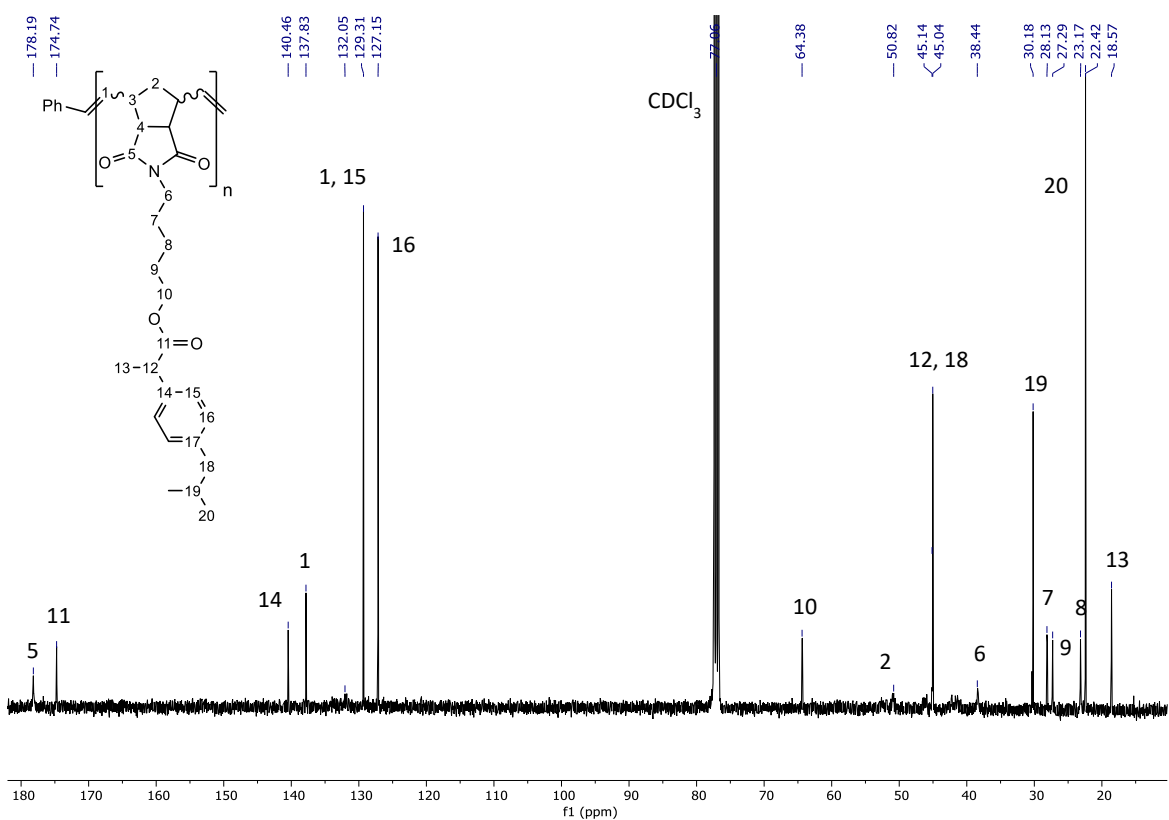


Fig. S23. ^1H NMR in CDCl_3 of homopolymer **poly5b**



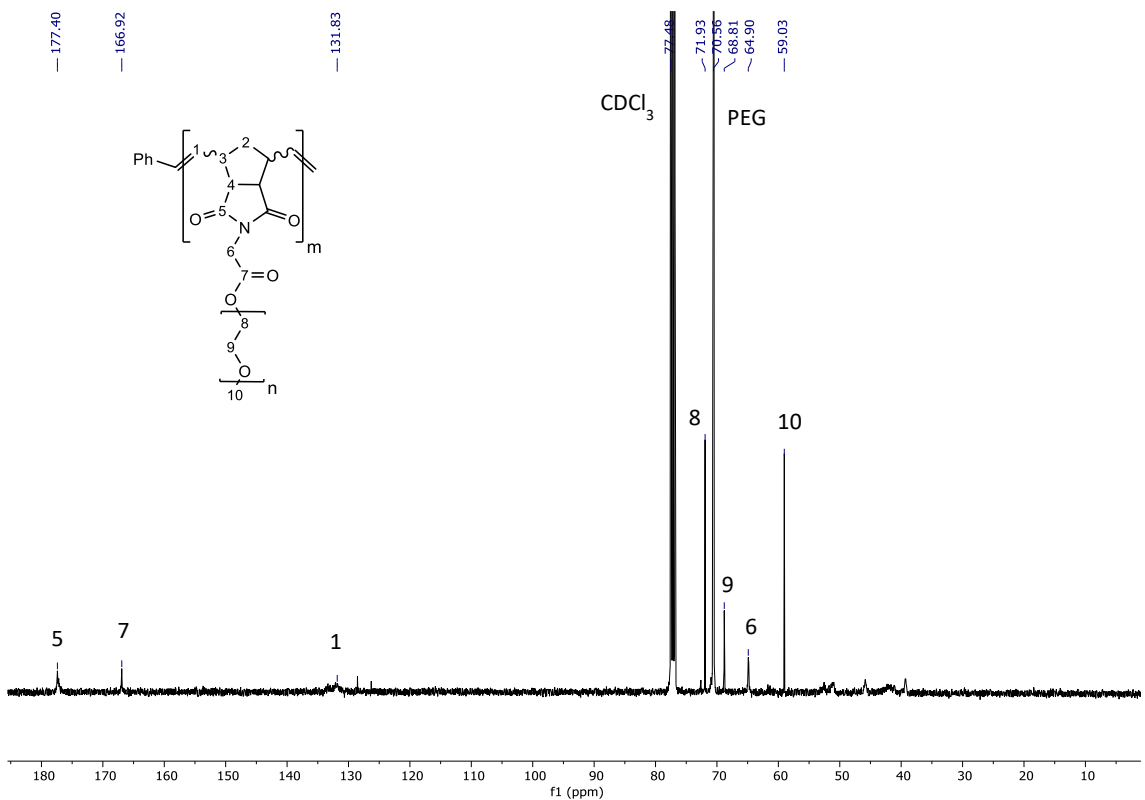


Fig. S26. ^{13}C NMR in CDCl_3 of homopolymer **poly10b**

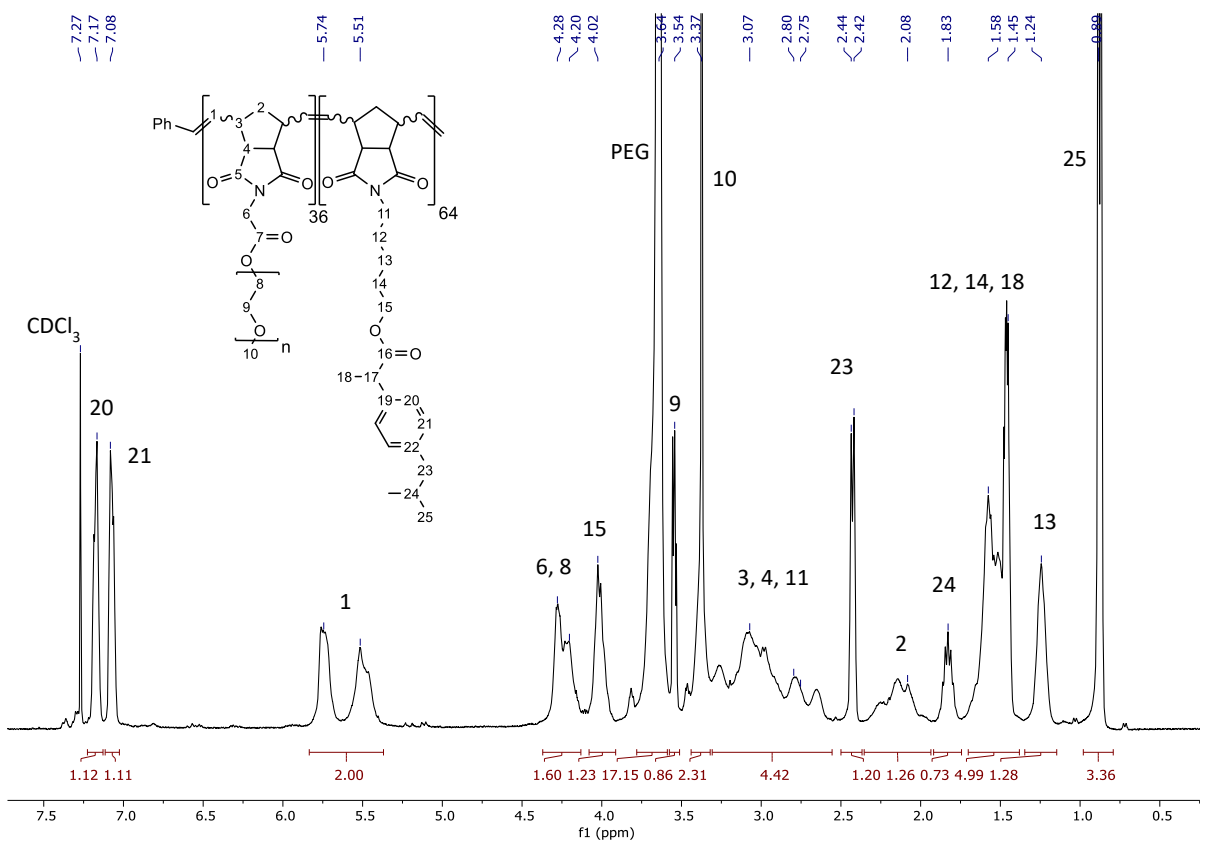
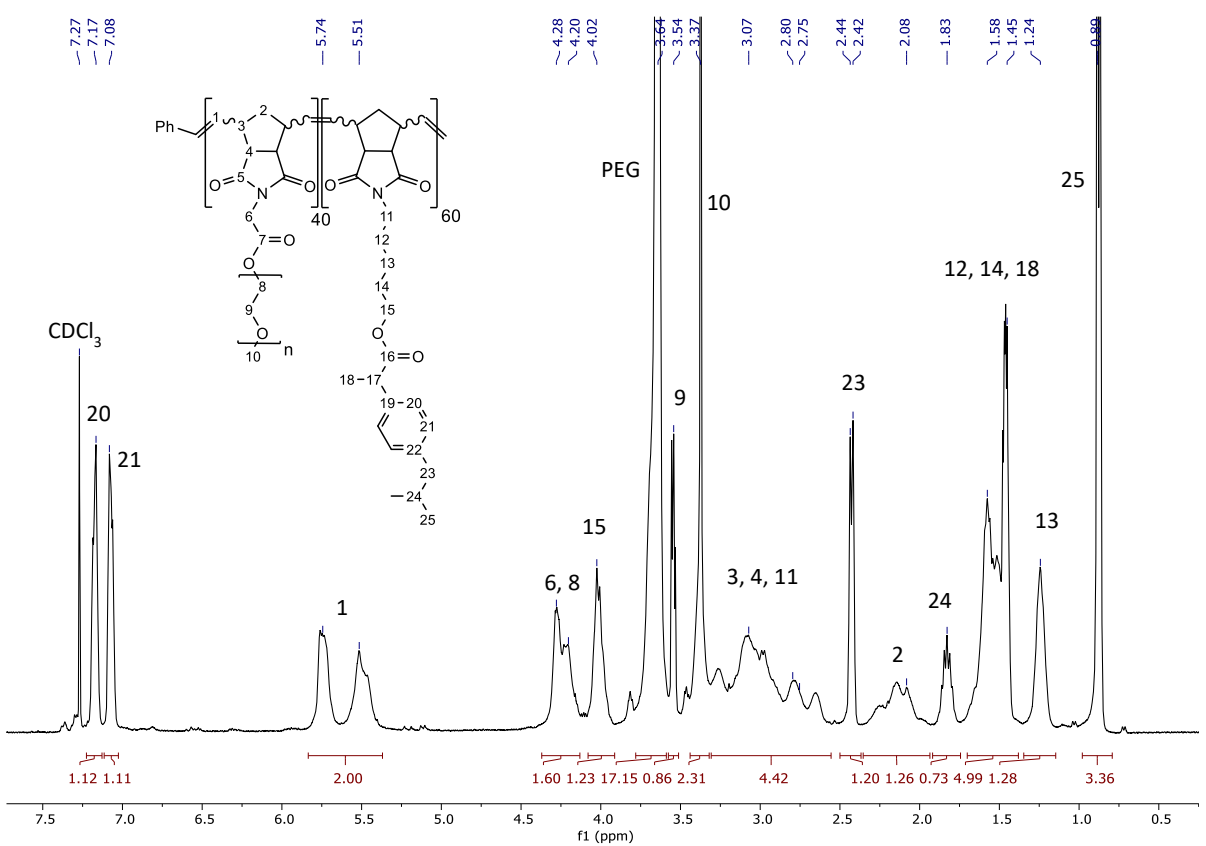
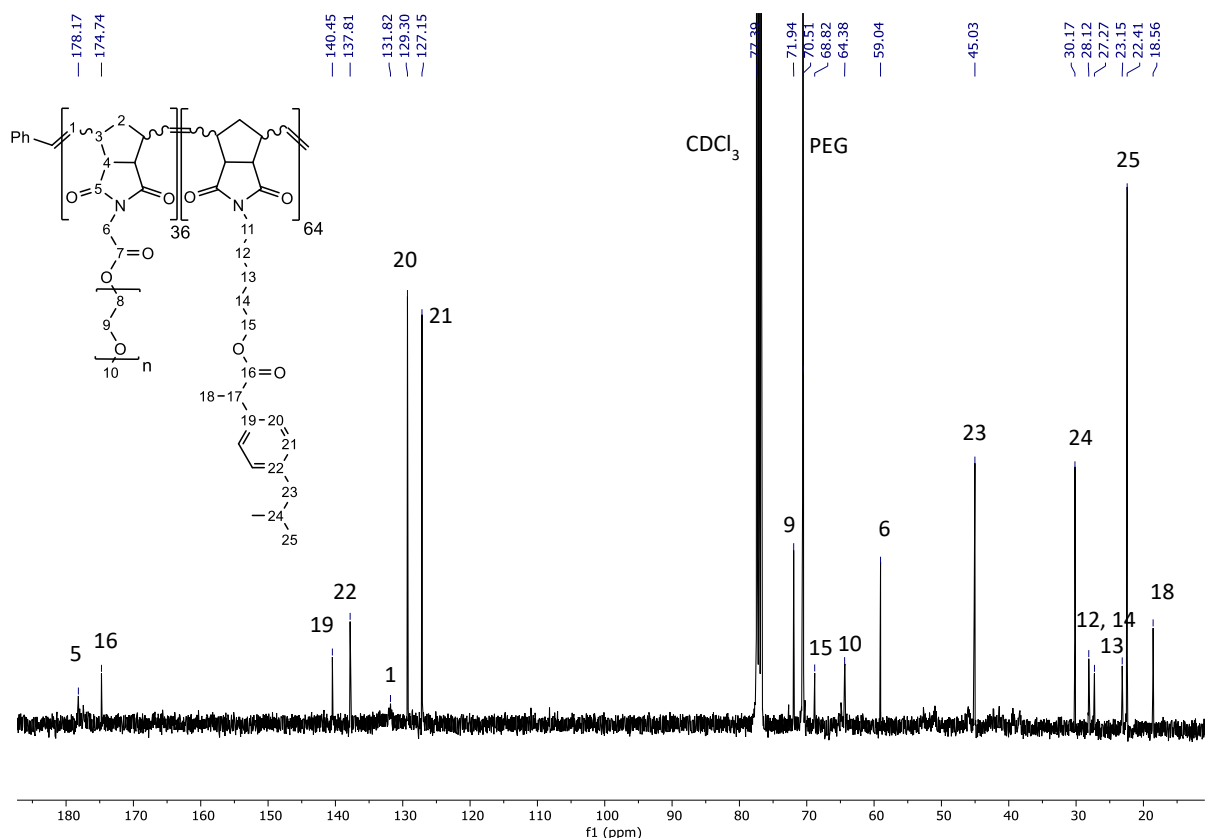


Fig. S27. ^1H NMR in CDCl_3 of block copolymer, **poly5b-b-poly10b [64:36]**



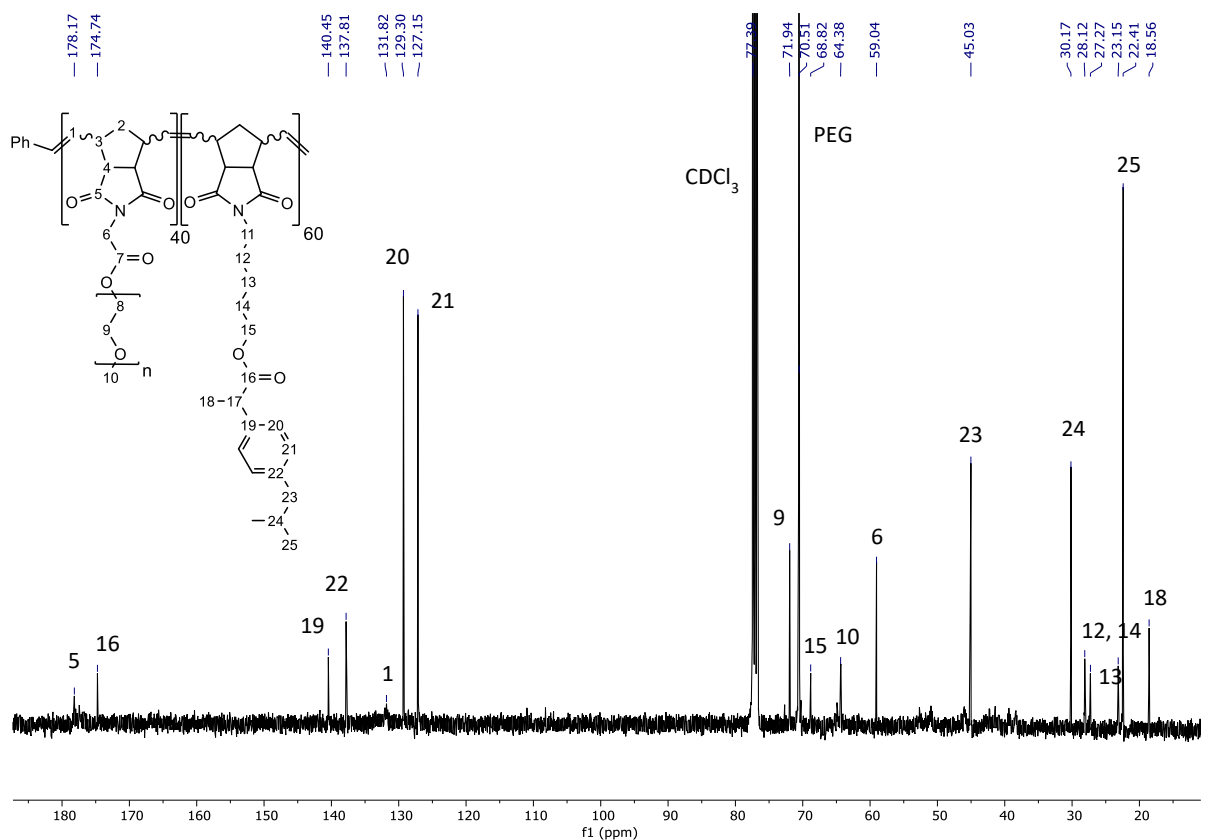


Fig. S30. ^{13}C NMR in CDCl_3 of statistical copolymer, **poly5b-co-poly10b [60:40]**

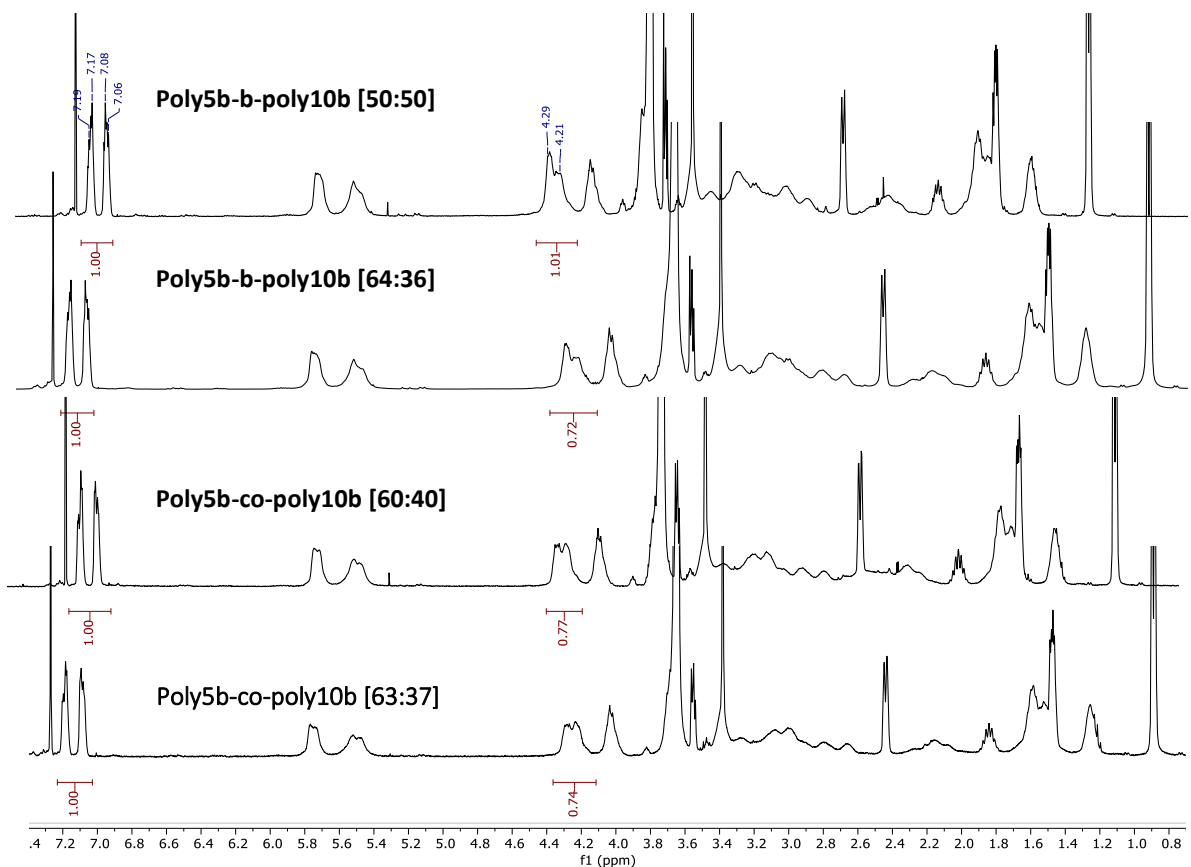


Fig. S31. Quantitative NMR analysis of block and statistical copolymers. The ratio between the highlighted integrals afforded the relative percentages of ibuprofen and PEG containing monomers (NB-Ibu/NB-PEG) within the polymer backbone of each polymer sequence.

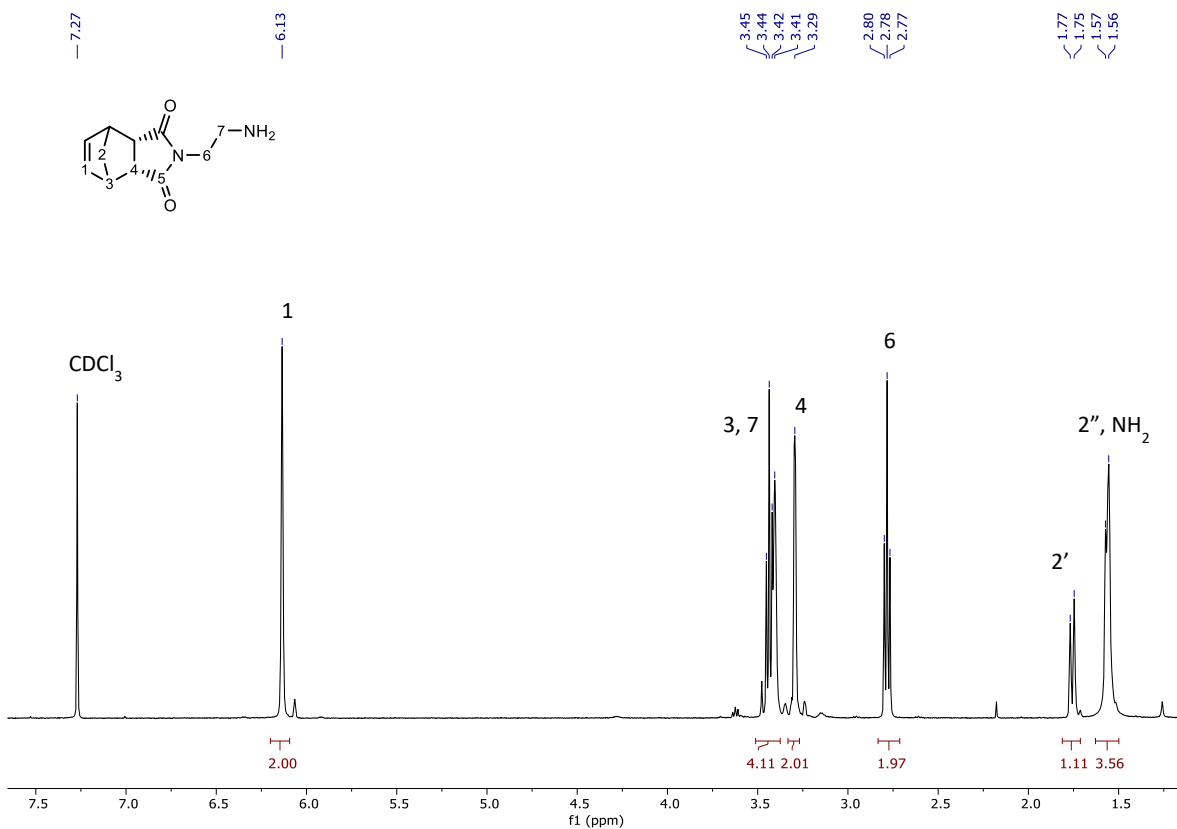


Fig. S32. ¹H NMR in CDCl₃ of *endo*-N-(2-aminoethyl)-5-norbornene-2,3-dicarboximide, **11**

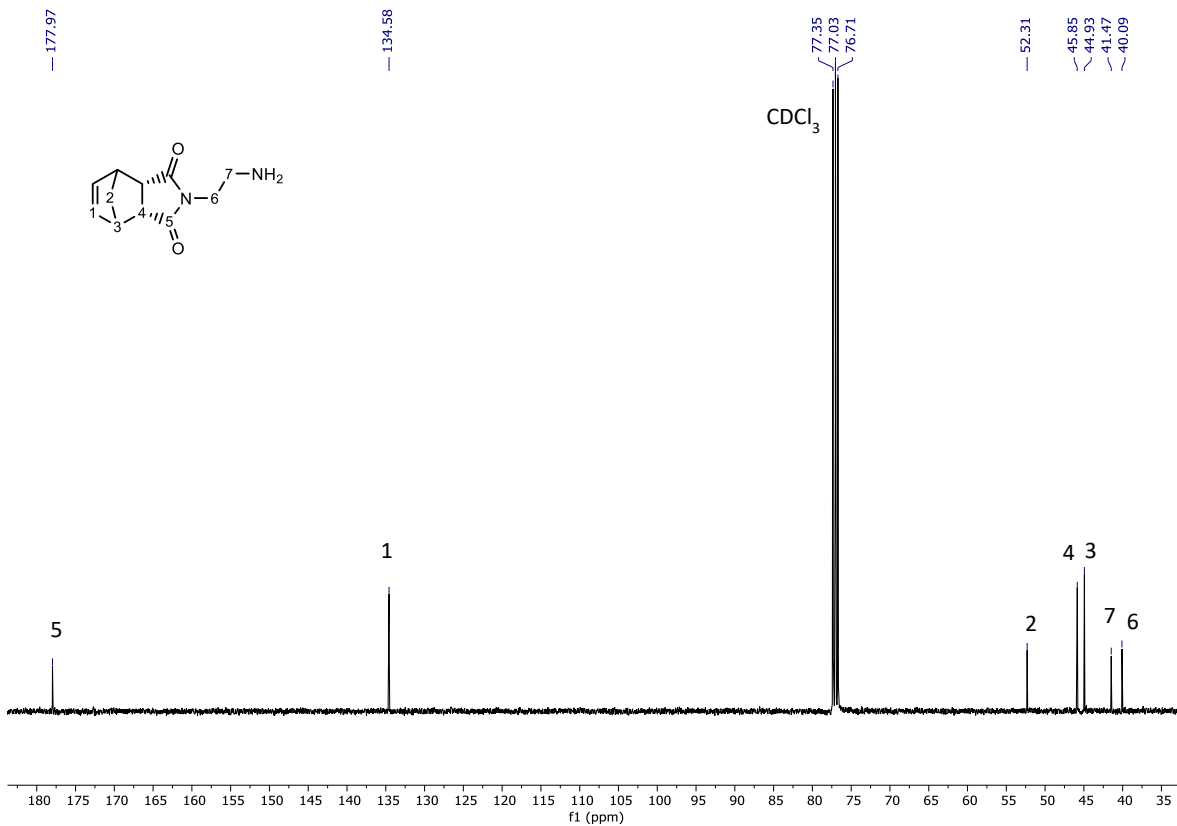


Fig. S33. ¹³C NMR in CDCl₃ of *endo*-N-(2-aminoethyl)-5-norbornene-2,3-dicarboximide, **11**

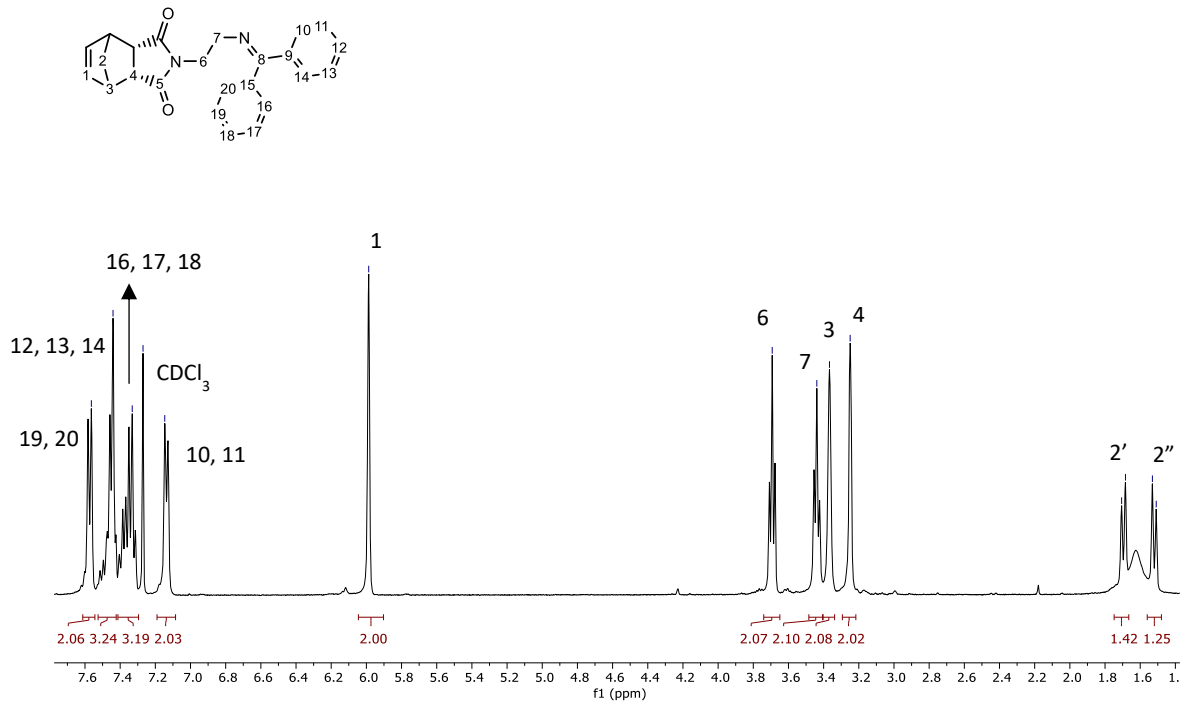


Fig. S34. ^1H NMR in CDCl_3 of compound **13a**

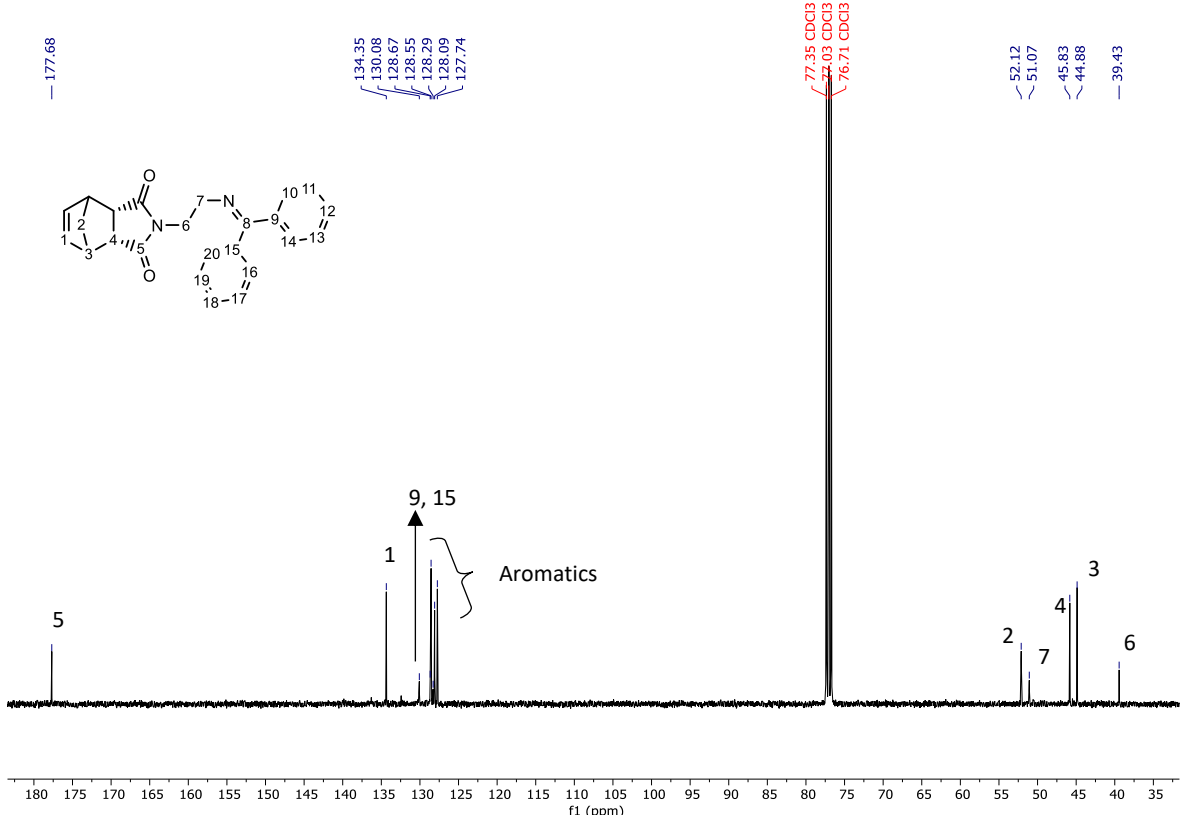


Fig. S35. ^{13}C NMR in CDCl_3 of compound **13a**

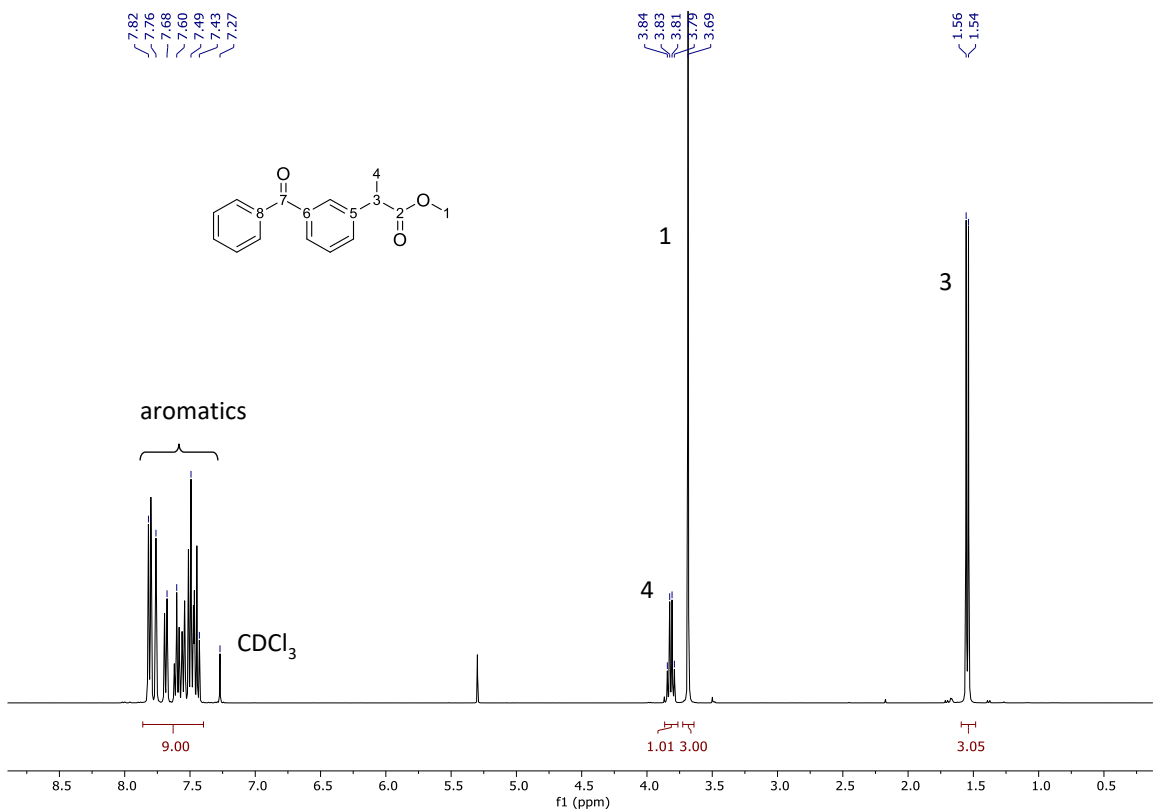


Fig. S36. ^1H NMR in CDCl_3 of ketoprofen ester, **12c**

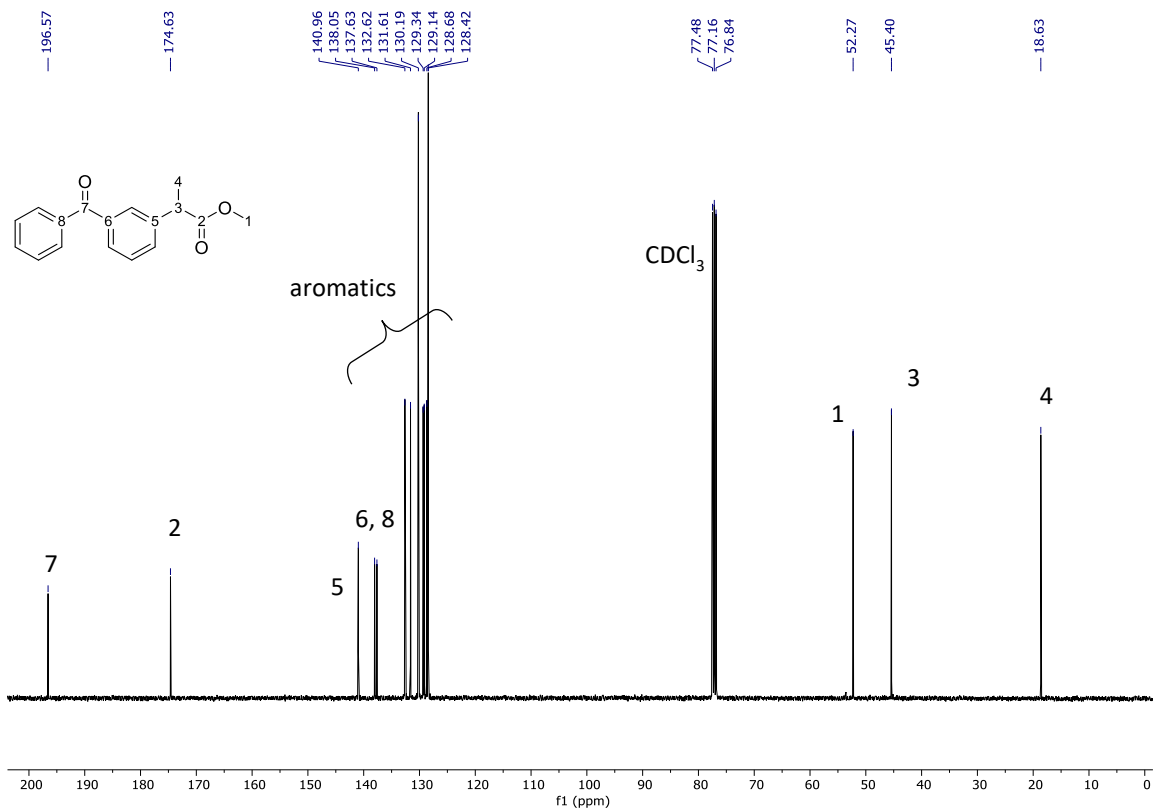


Fig. S37. ^{13}C NMR in CDCl_3 of ketoprofen ester, **12c**

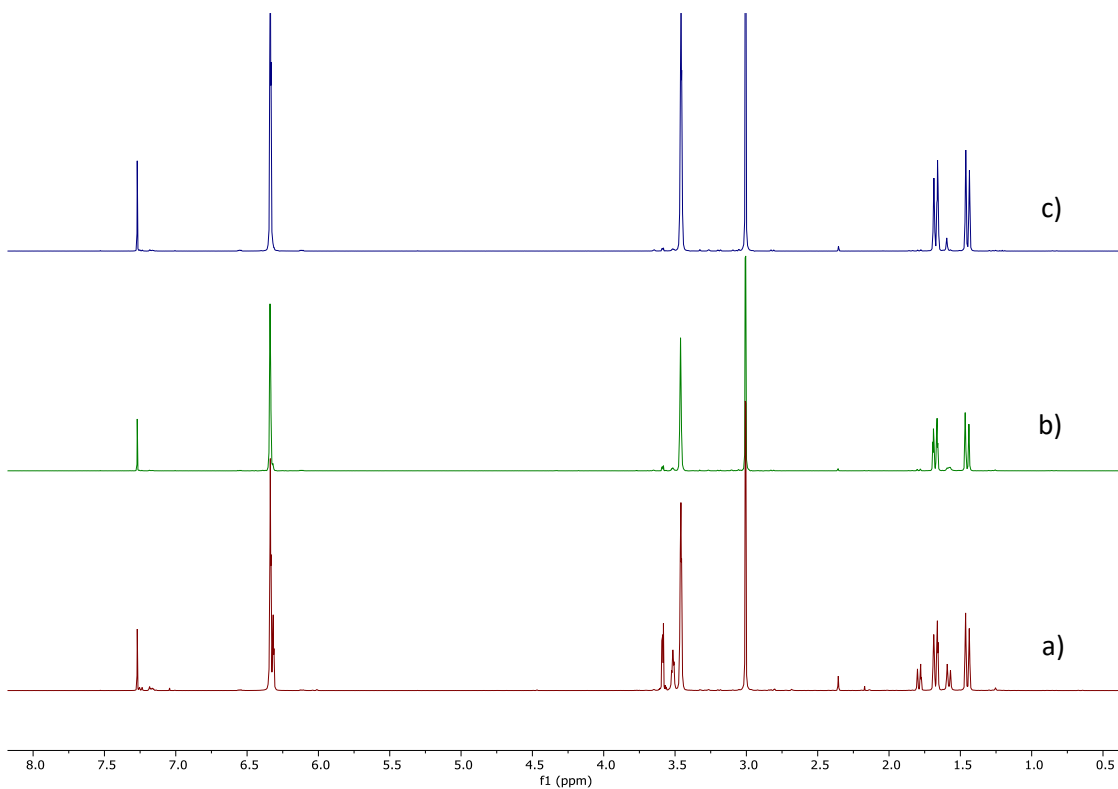


Fig. S38. Stacked ¹H NMR in CDCl₃ of endo/exo carbic anhydride conversion. a) 1st recrystallisation afforded exo-carbic anhydride with 78 % purity; b) 2nd recrystallisation with 97 % of exo purity; c) 3rd recrystallisation with 99 % of exo purity. The purity of exo carbic anhydride is calculated by the integration of the bridgehead protons of endo and exo between 2.0 ppm and 1.25 ppm.

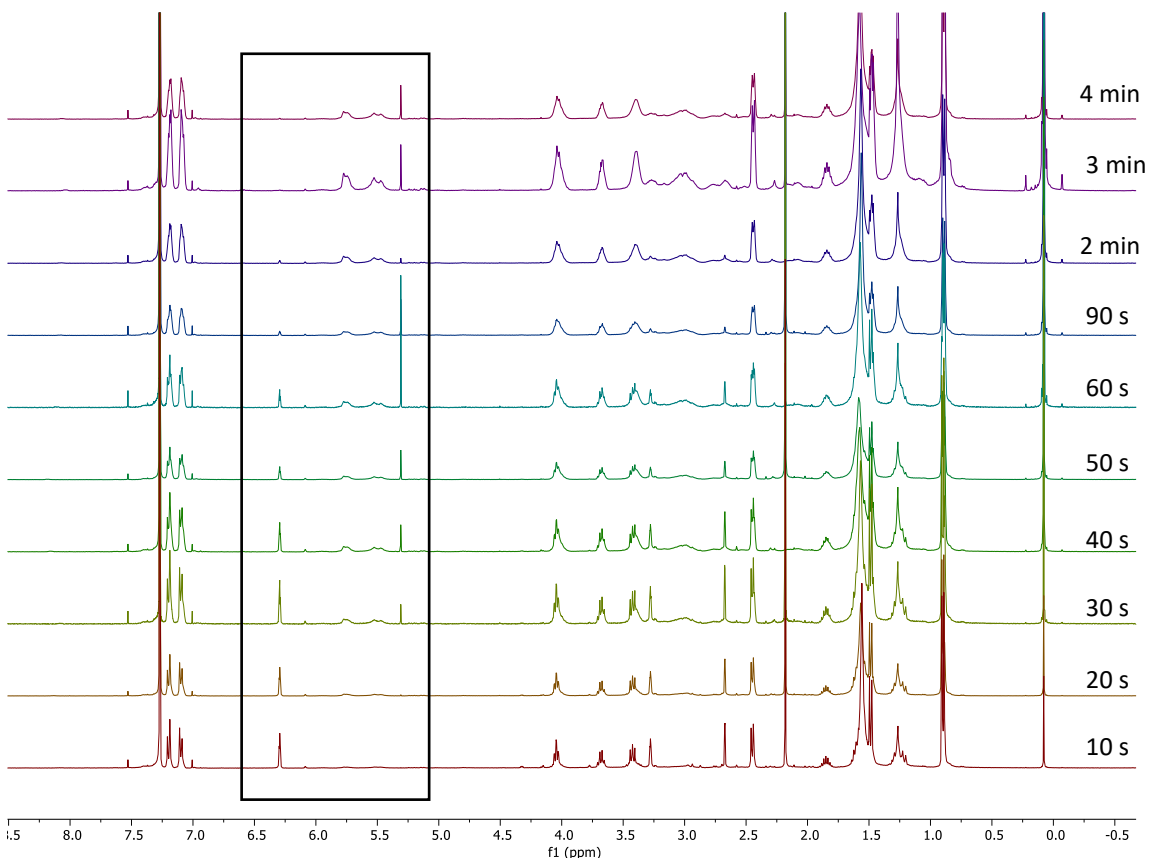


Fig. S39. Stacked ¹H NMR spectra in CDCl₃ showing monomer **5b** conversion into homopolymer **poly5b**.

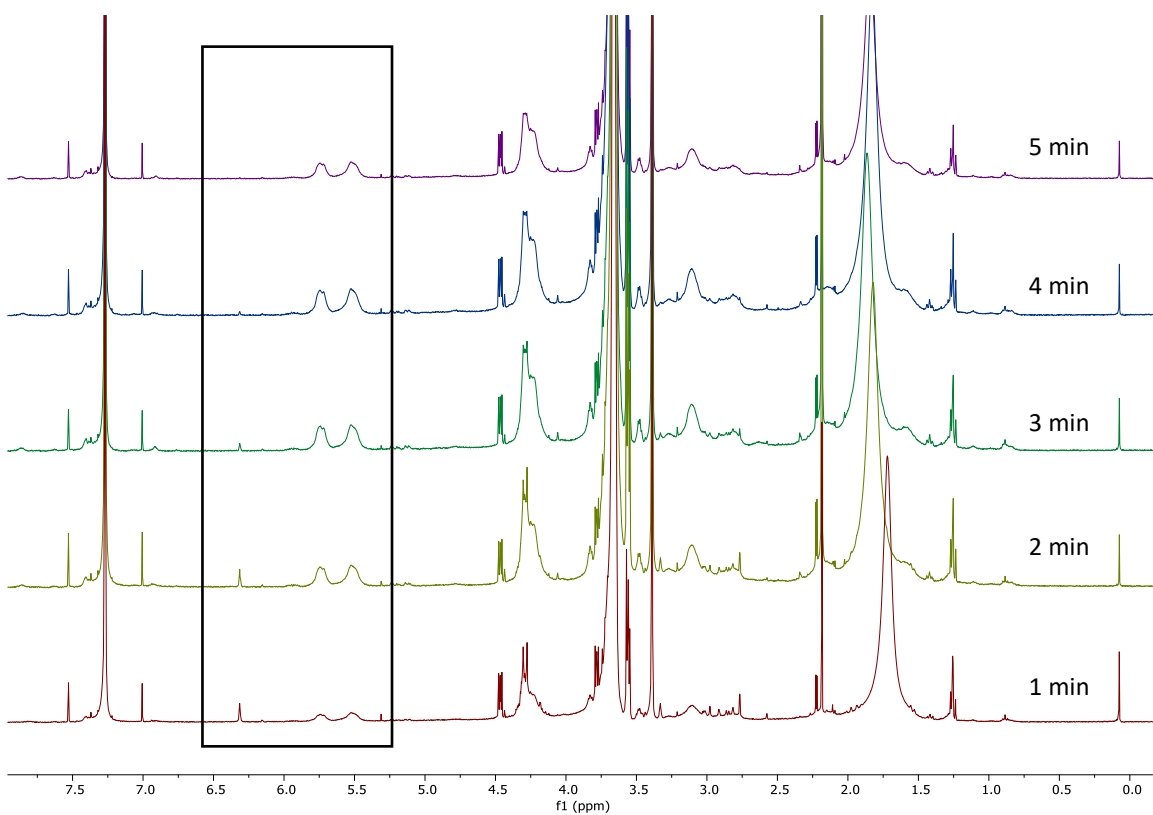


Fig. S40. Stacked ^1H NMR spectra in CDCl_3 showing monomer **10b** conversion into homopolymer **poly10b**.

2. LC-MS spectra

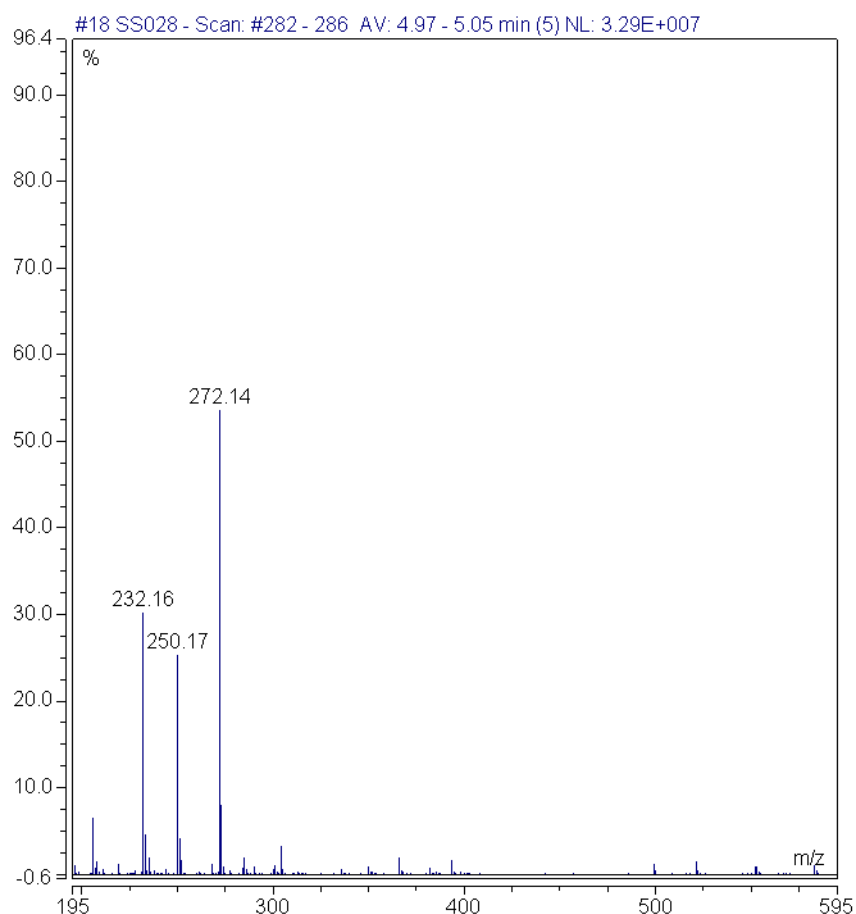


Fig. S41. LC-MS spectra of compound **3b**. Here are identified the $[M+H]^+$ and $[M+Na]^+$ values, 250.2 and 272.1 respectively.

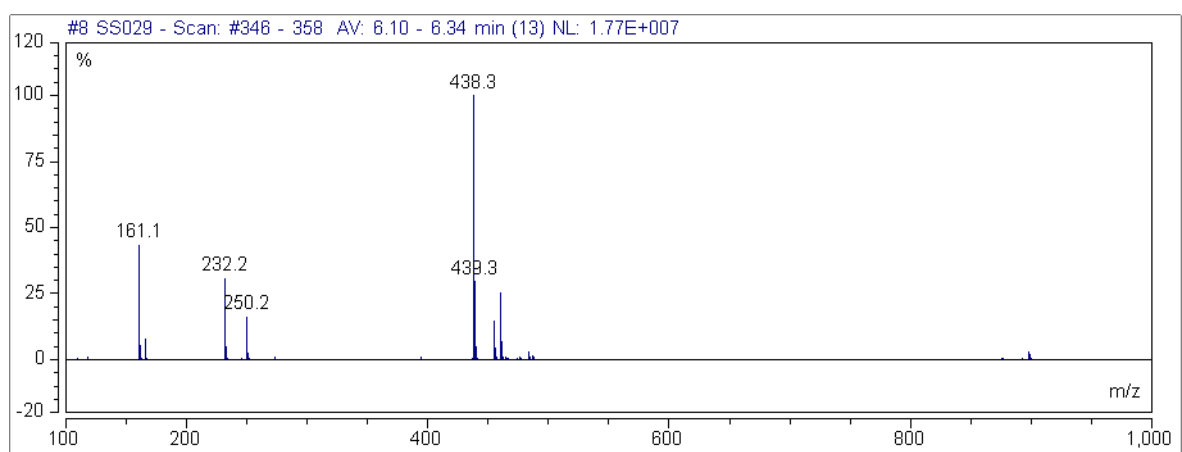


Fig. S42. LC-MS spectra of compound **5b**. Here the $[M+H]^+$ value of 438.3 is identified.

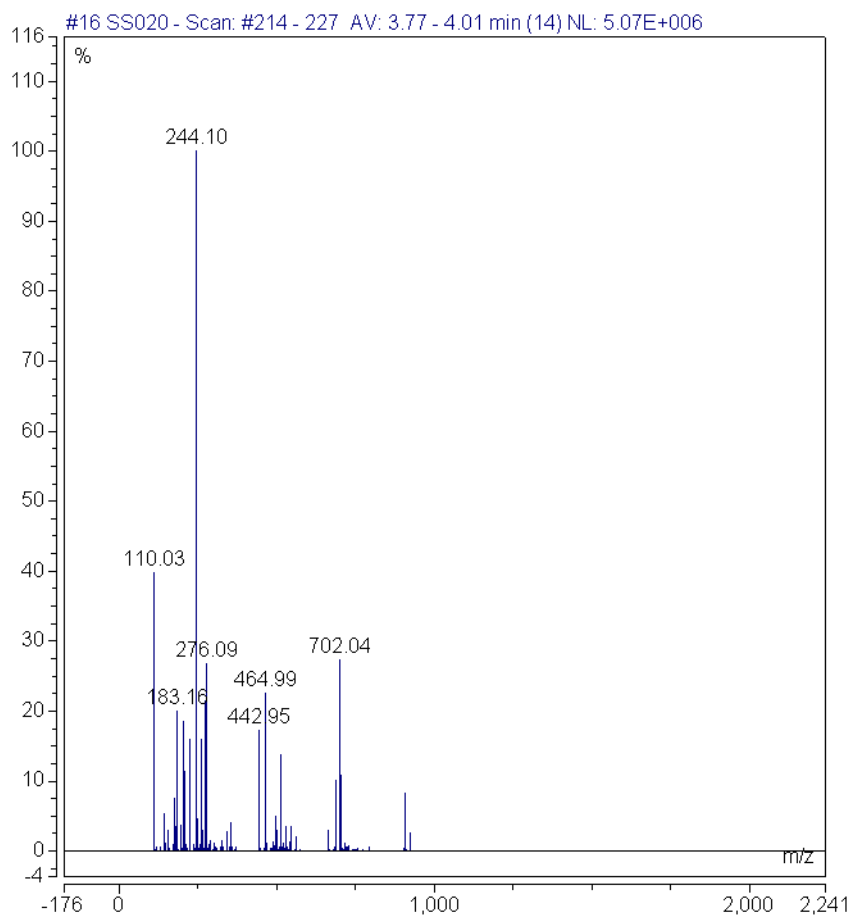


Fig. S43. LC-MS spectra of compound **7b**. Here the $[M+Na]^+$ value is identified, 244.1.

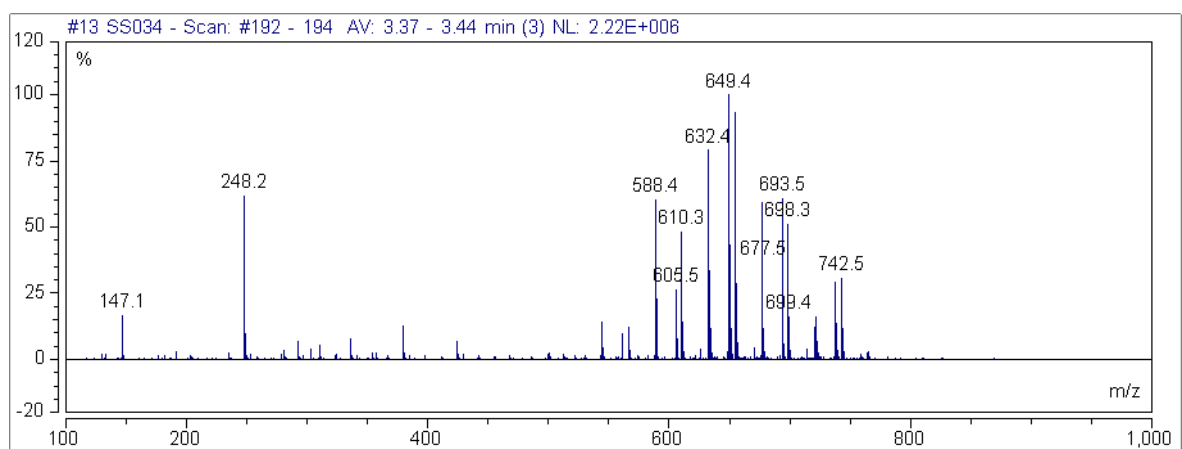


Fig. S44. LC-MS spectra of monomer **10b**. Due to the presence of a PEG chain to the norbornene moiety, a distribution of m/z is obtained.

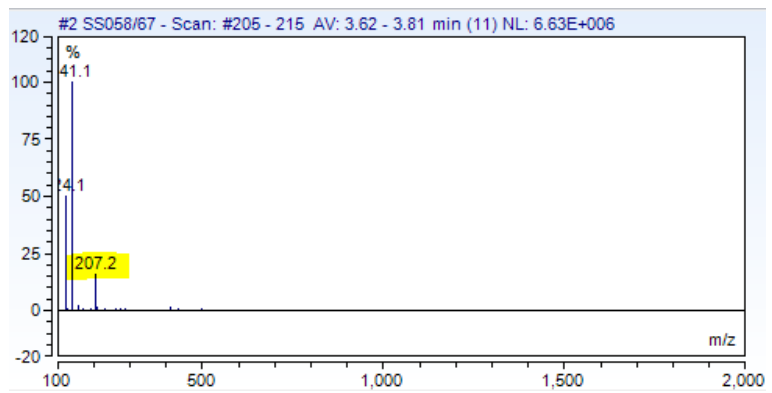


Fig. S45. LC-MS spectra of compound **11**. Here the $[M+H]^+$ value is identified, 207.2.

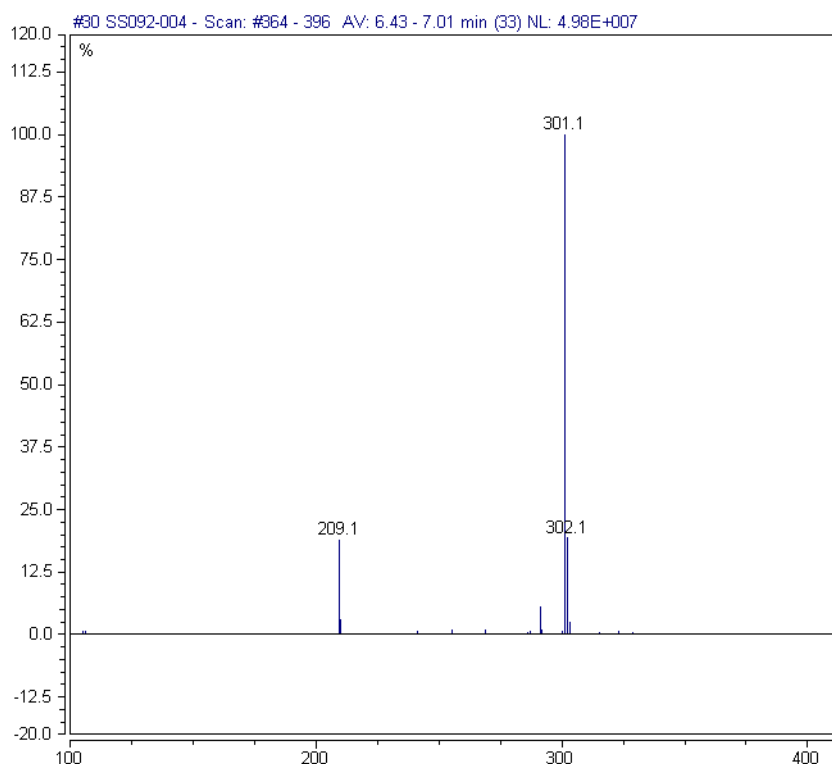


Fig. S46. LC-MS spectra of compound **12c**. Here the $[M+H]^+$ value is identified, 301.1.

3. IR spectra

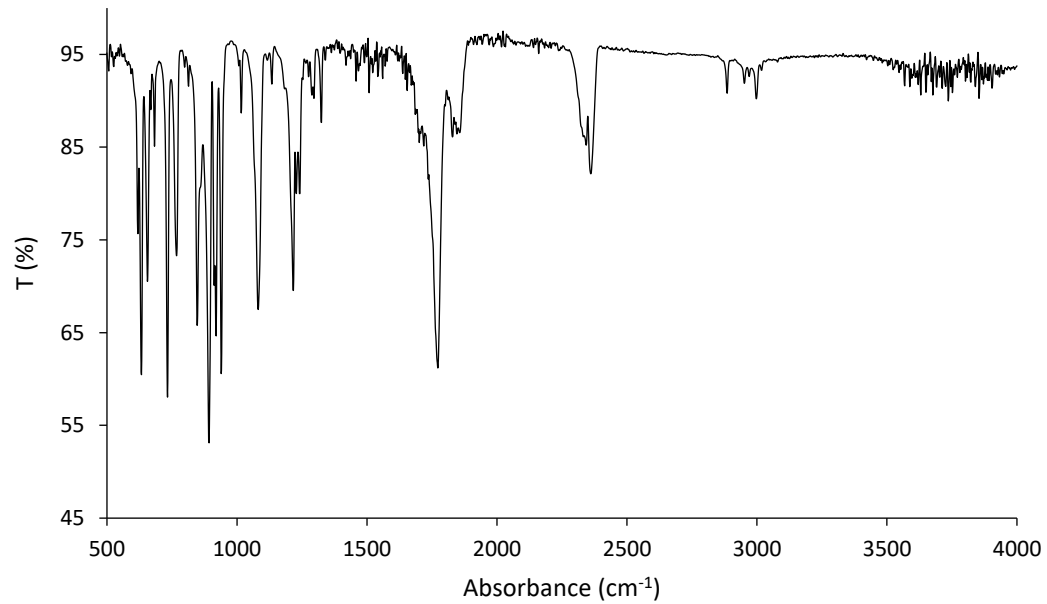


Fig. S47. IR spectra of exo-carbic anhydride, **1b**

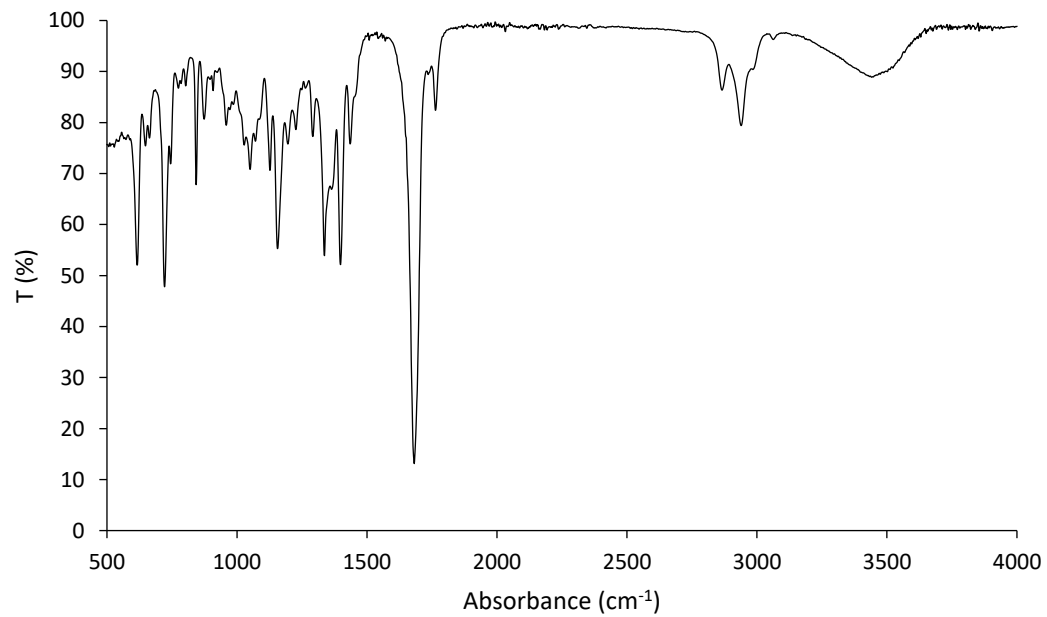


Fig. S48. IR spectra of *N*-(hydroxypentanyl)-*cis*-5-norbornene-*endo*-2,3-dicarboximide, **3a**

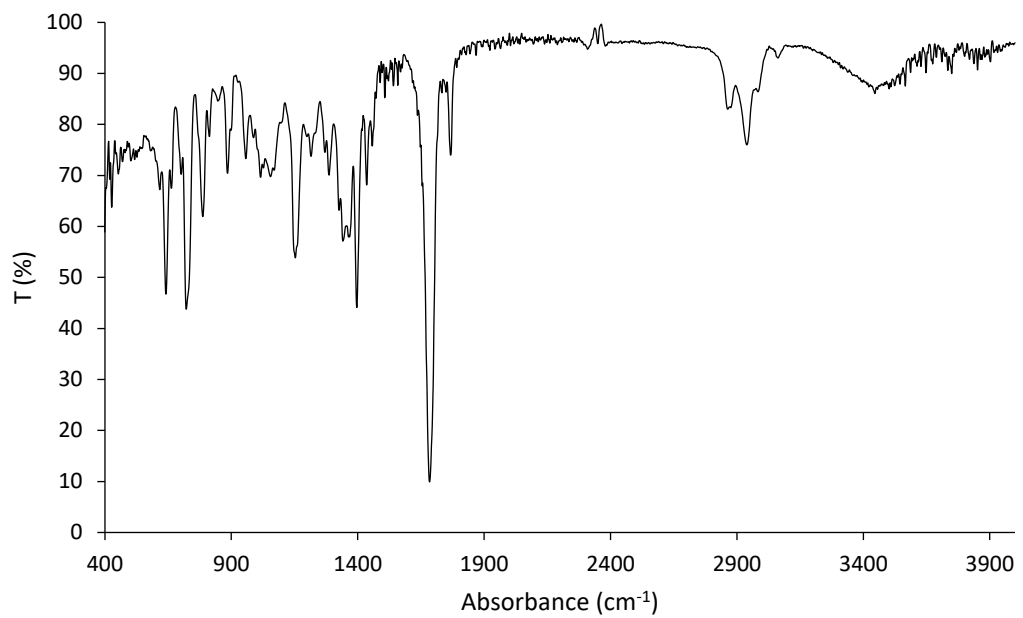


Fig. S49. IR spectra of *N*-(hydroxypentanyl)-*cis*-5-norbornene-*exo*-2,3-dicarboximide, **3b**

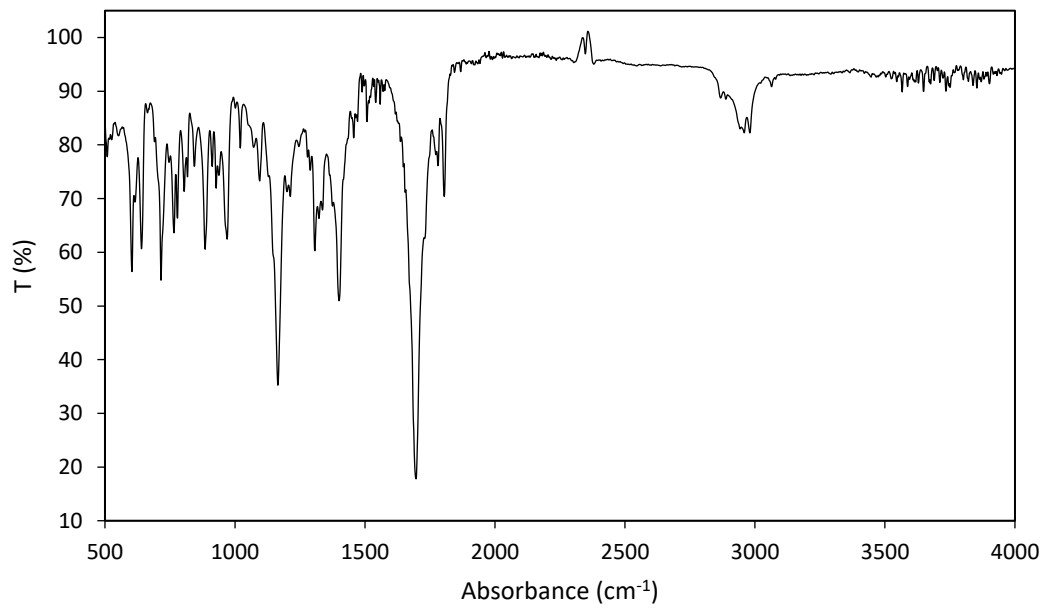


Fig. S50. IR spectra of *endo*-NB ibuprofen derivative, **5a**

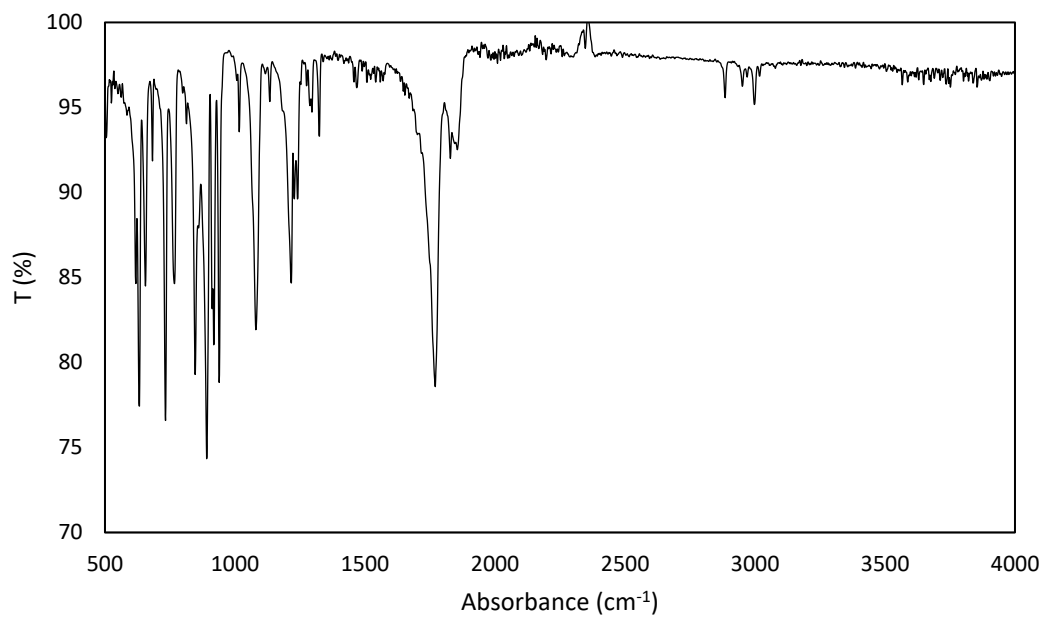


Fig. S51. IR spectra of NB-IBU monomer **5b**

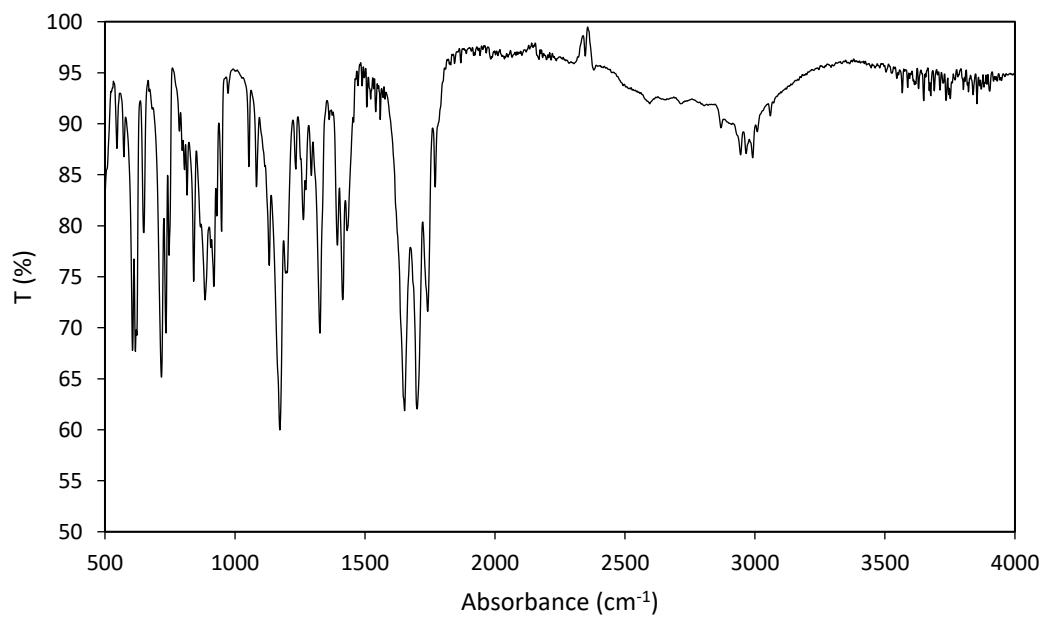


Fig. S52. IR spectra of *N*-(*endo*-himoyl)-glycine, **7a**

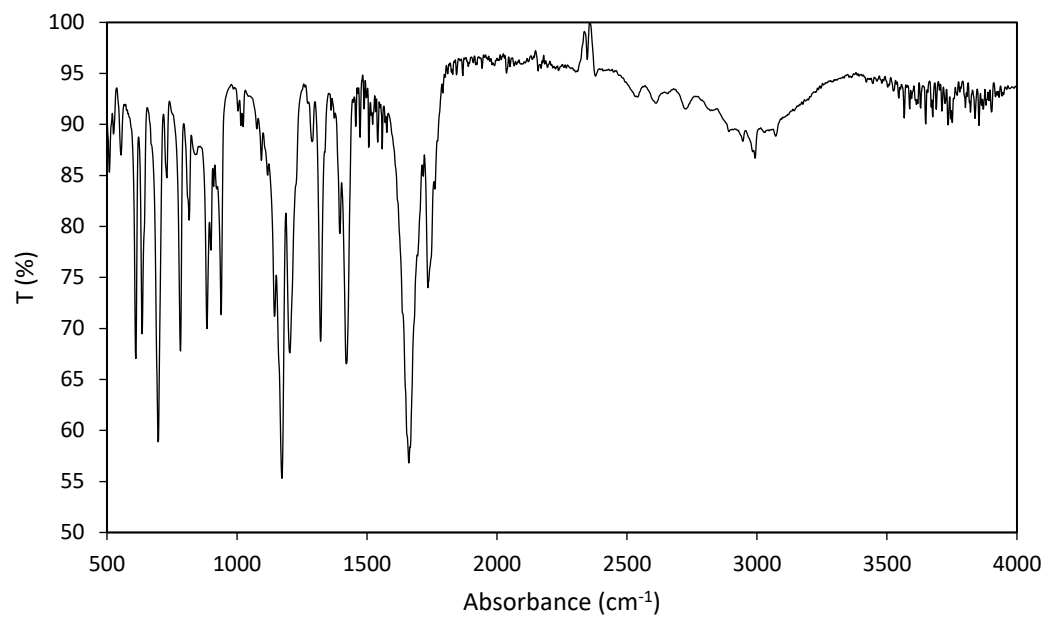


Fig. S53. IR spectra of *N*-(*exo*-himoyl)-glycine, **7b**

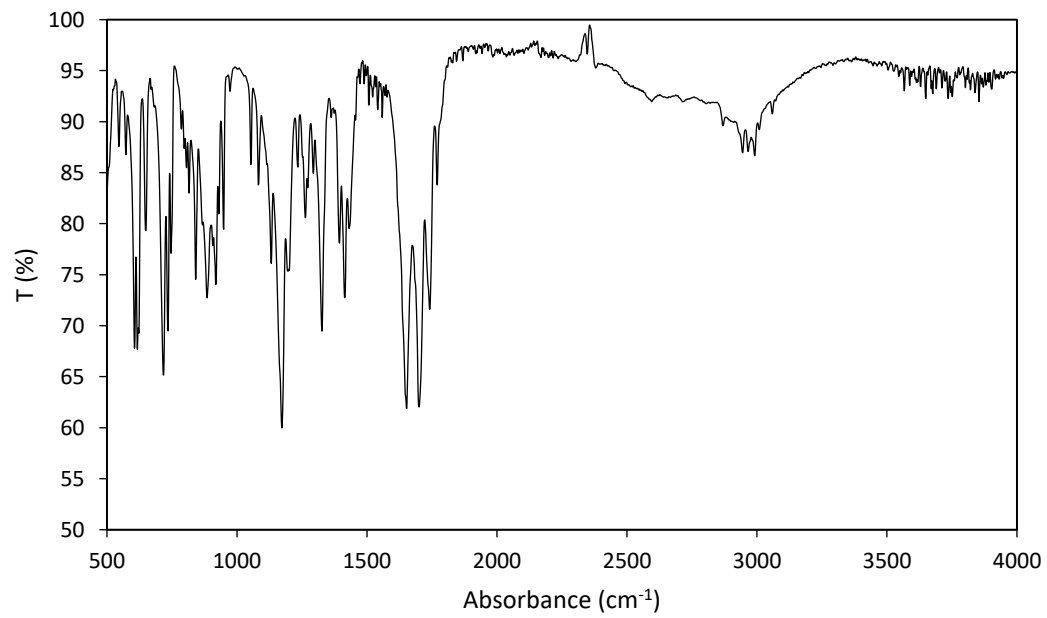


Fig. S54. IR spectra of *N*-(*endo*-himoyl)-glycinoyl chloride, **8a**

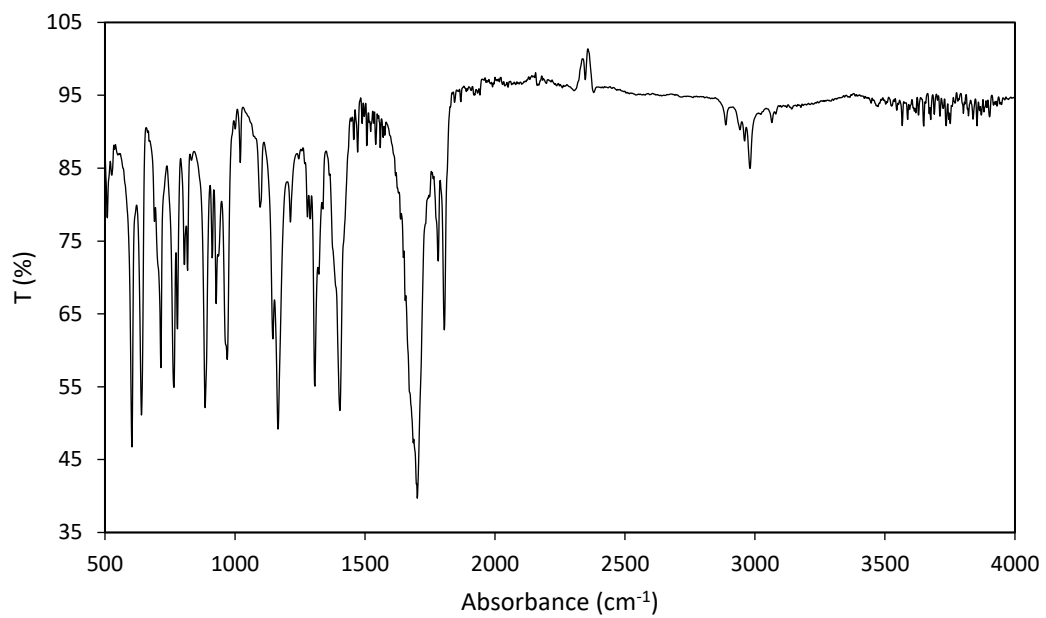


Fig. S55. IR spectra of *N*-(*exo*-himoyl)-glycinoyl chloride, **8b**

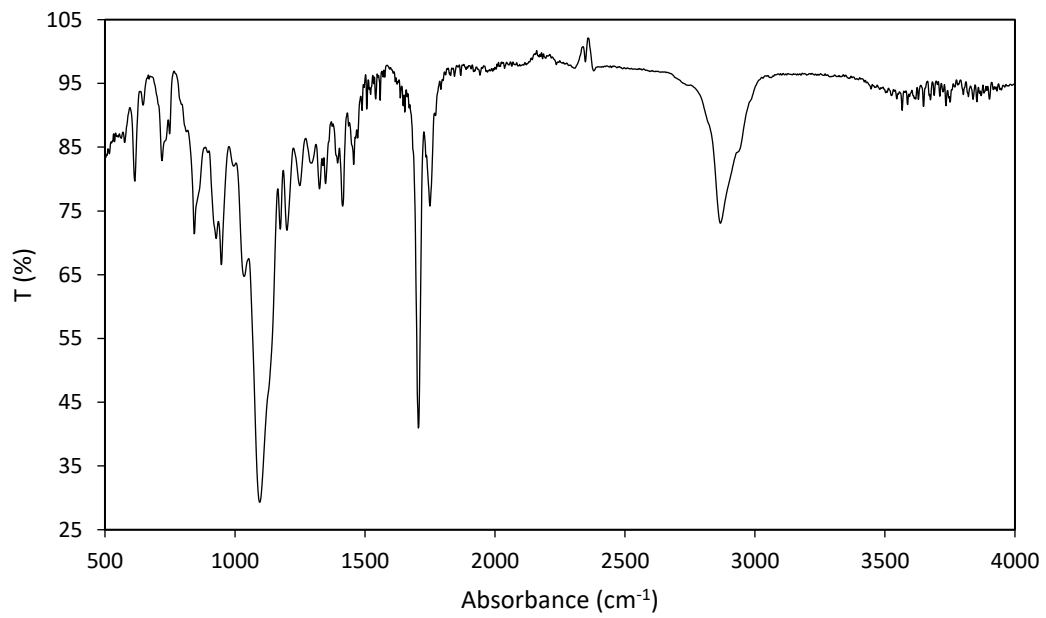


Fig. S56. IR spectra of *N*-(*endo*-himoyl)-glycine poly(ethylene glycol) ester, **10a**

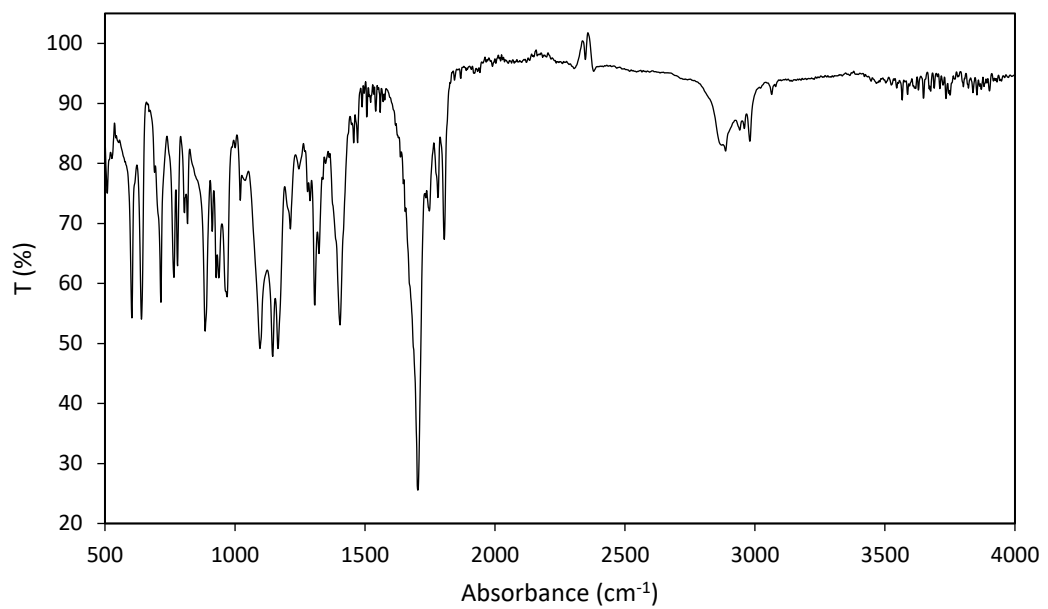


Fig. S57. IR spectra of *N*-(*exo*-himoyl)-glycine poly(ethylene glycol) ester, NB-PEG monomer **10b**

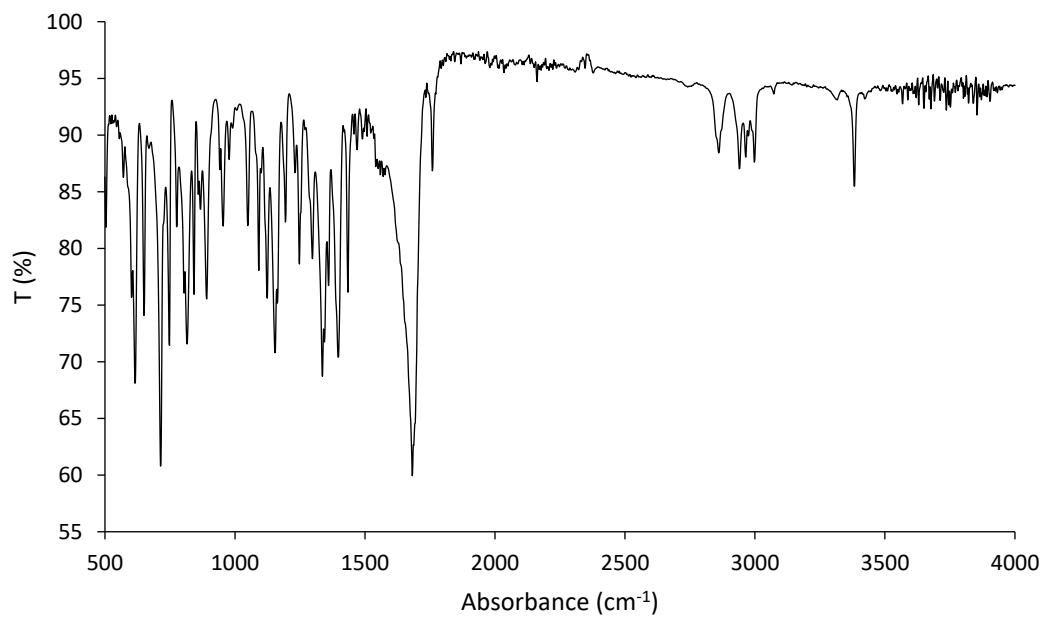


Fig. S58. IR spectra of *endo*-*N*-(2-aminoethyl)-5-norbornene-2,3-dicarboximide, **11**

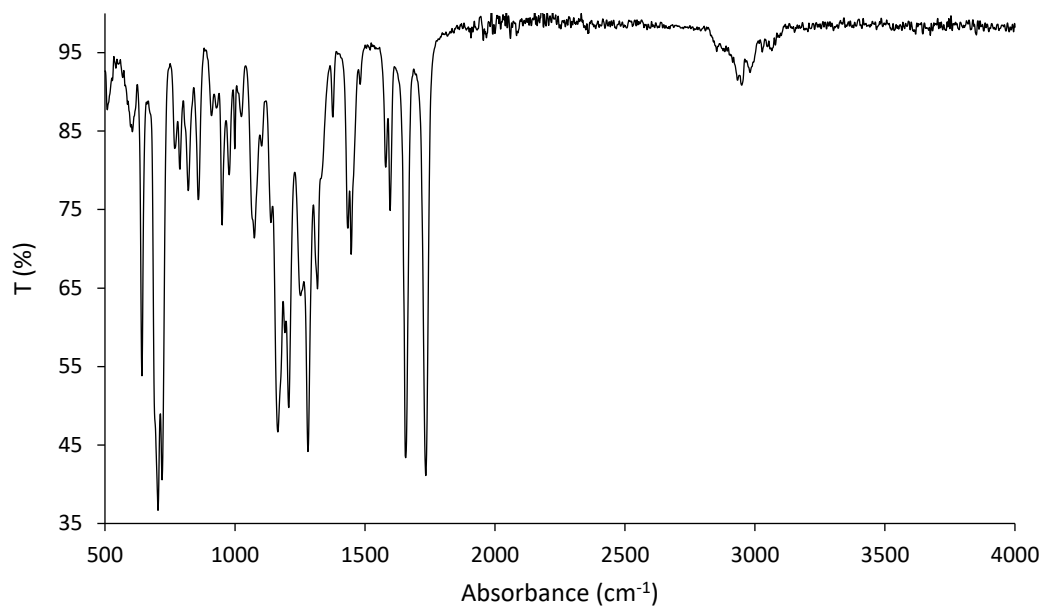


Fig. S59. IR spectra of ketoprofen ester, **12c**

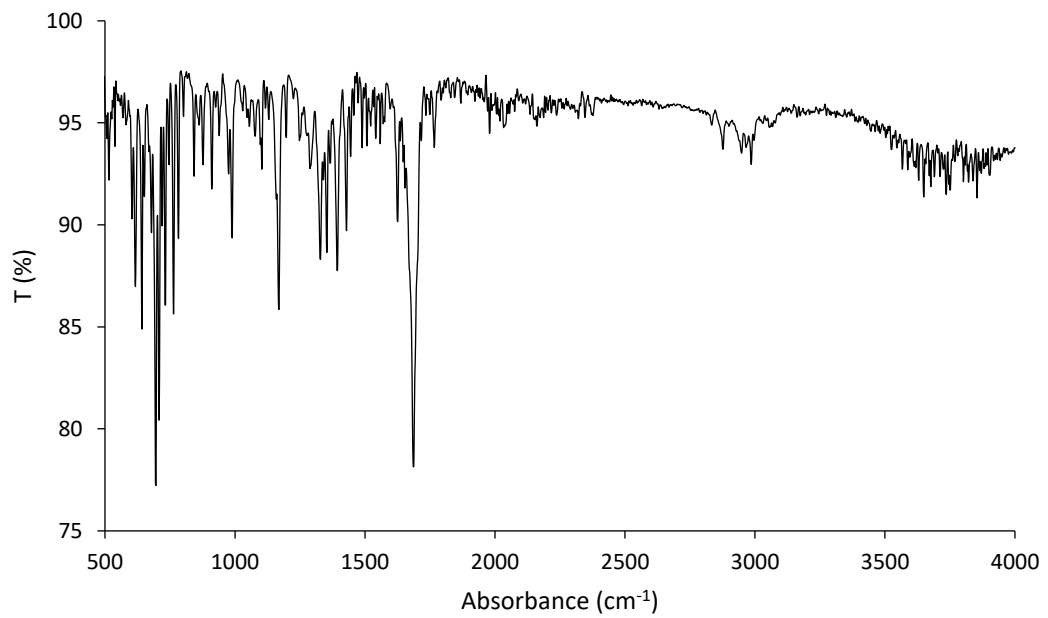


Fig. S60. IR spectra of *endo*-(2-diphenyl imine)-ethyl-5-norbornene-2,3-dicarboximide, **13a**

4. GC chromatograms of *endo/exo* isomerisation

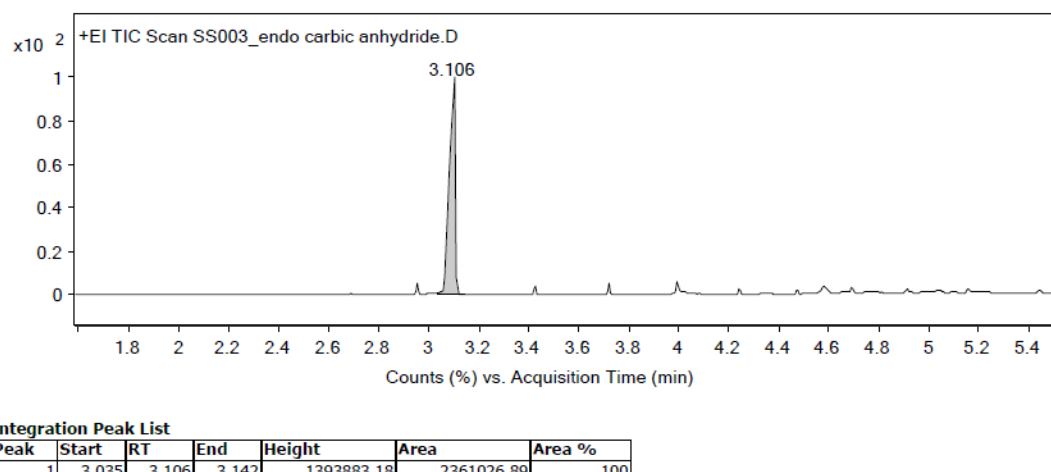


Fig. S61. GC chromatogram of *endo*-carbic anhydride **1a**

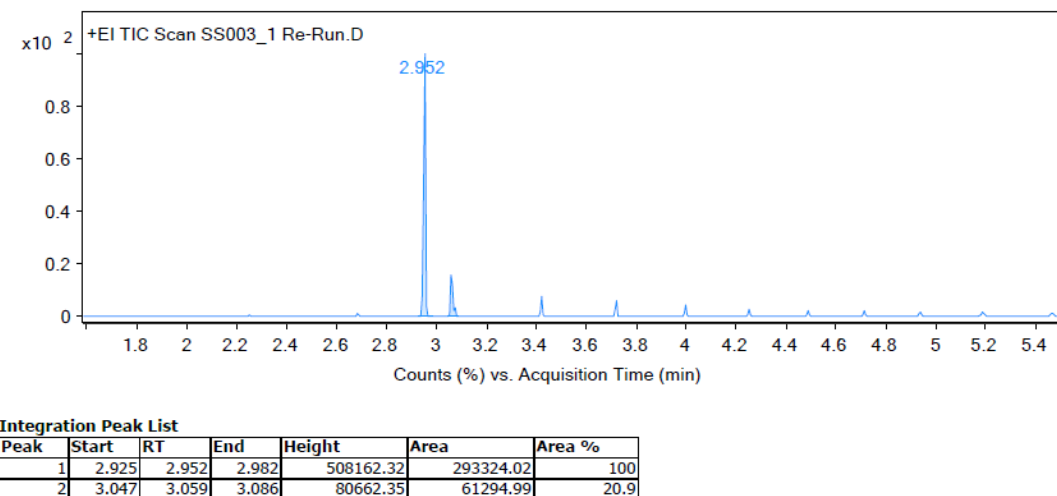


Fig. S62. GC chromatogram of crude of reaction containing 83 % *exo* adduct and 17 % *endo* adduct.

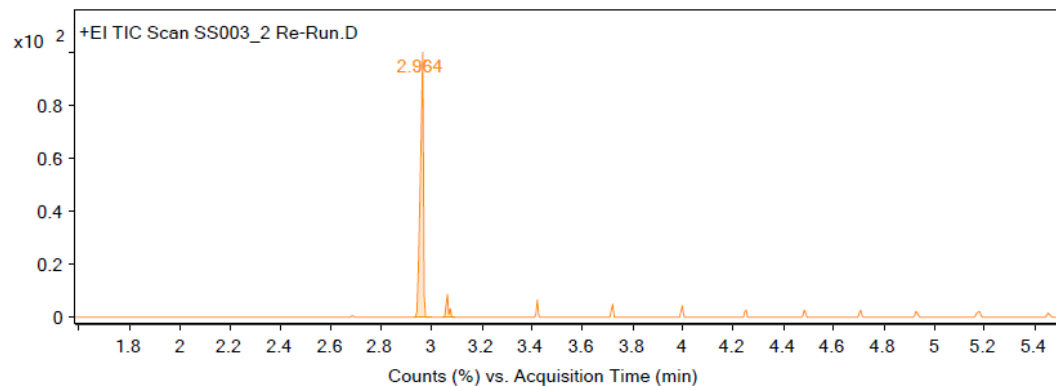


Fig. S63. GC chromatogram of first recrystallisation. *Exo*-carbic anhydride is 93 % pure.

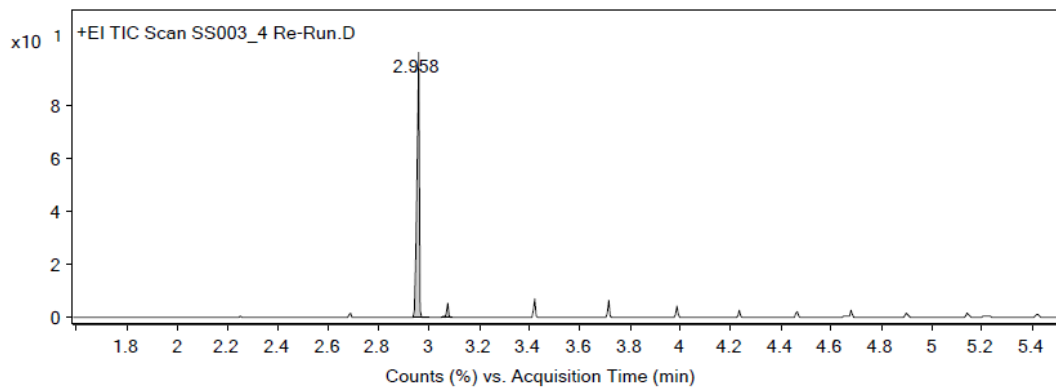


Fig. S64. GC chromatogram of second recrystallisation. *Exo*-carbic anhydride is 96 % pure.

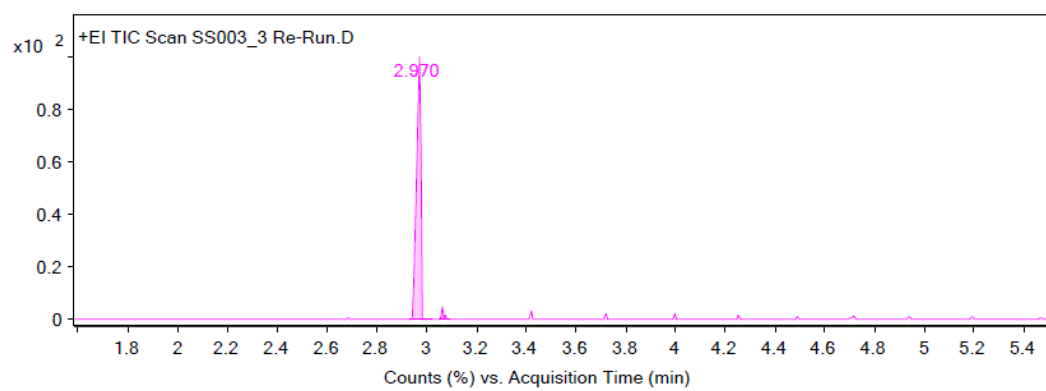


Fig. S65. GC chromatogram of third recrystallisation. *Exo*-carbic anhydride is 98 % pure.

5. Dynamic light scattering (DLS) of block and statistical copolymers

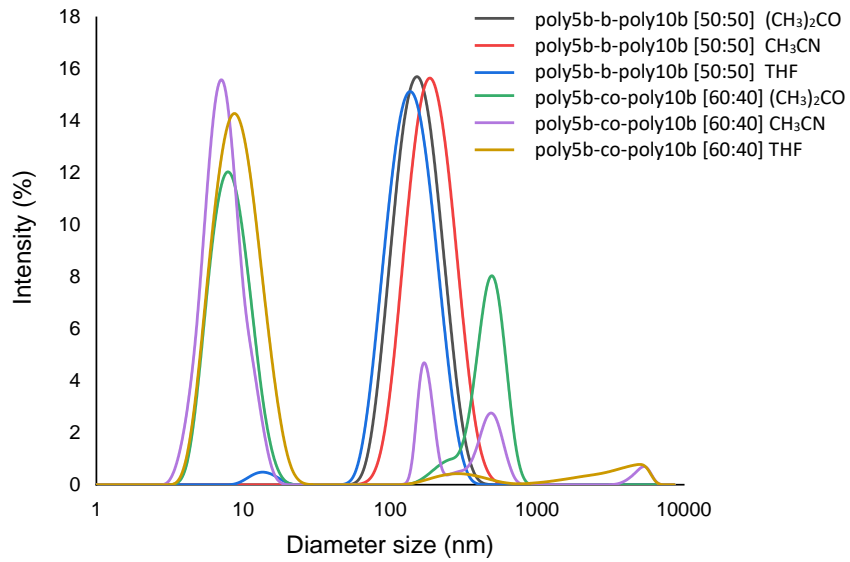


Fig. S66. DLS data of **poly5b-b-poly10b [50:50]** and **poly5b-co-poly10b [60:40]** self-assembled in different organic solvents such as acetonitrile, acetone and THF.

6. Transmission electron microscopy (TEM) images of block and statistical copolymers

6.1. Poly5b-b-poly10b [50:50] in acetonitrile

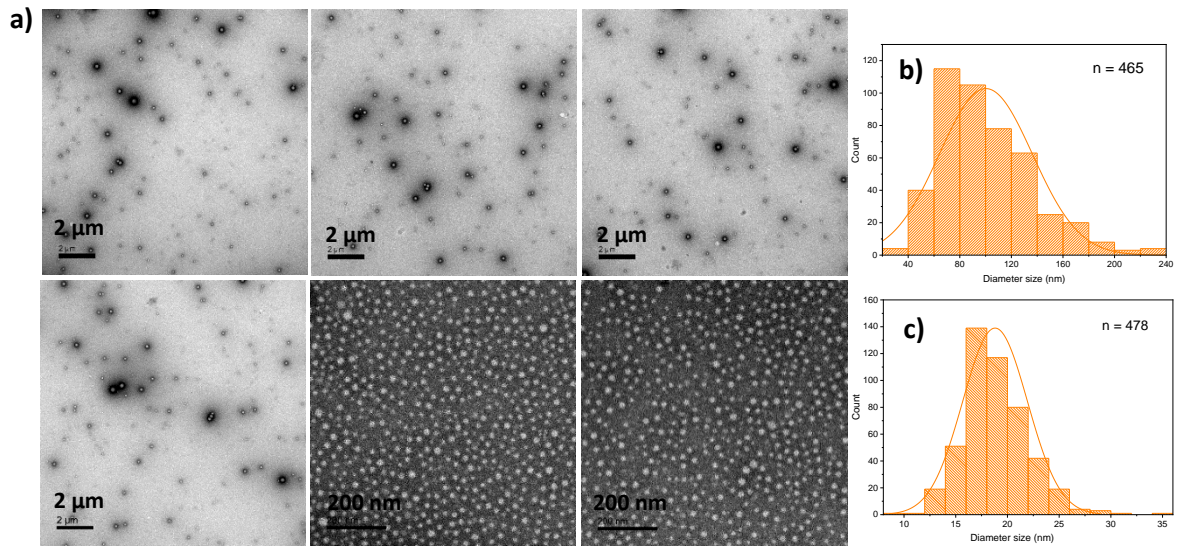


Fig. S67. a) TEM images of **poly5b-b-poly10b [50:50]** self-assembled in acetonitrile; b) distribution of bigger particles with average size (100 ± 36) nm; c) distribution of smaller particles with average size (19 ± 3) nm.

6.2. Poly5b-b-poly10b [50:50] in acetone

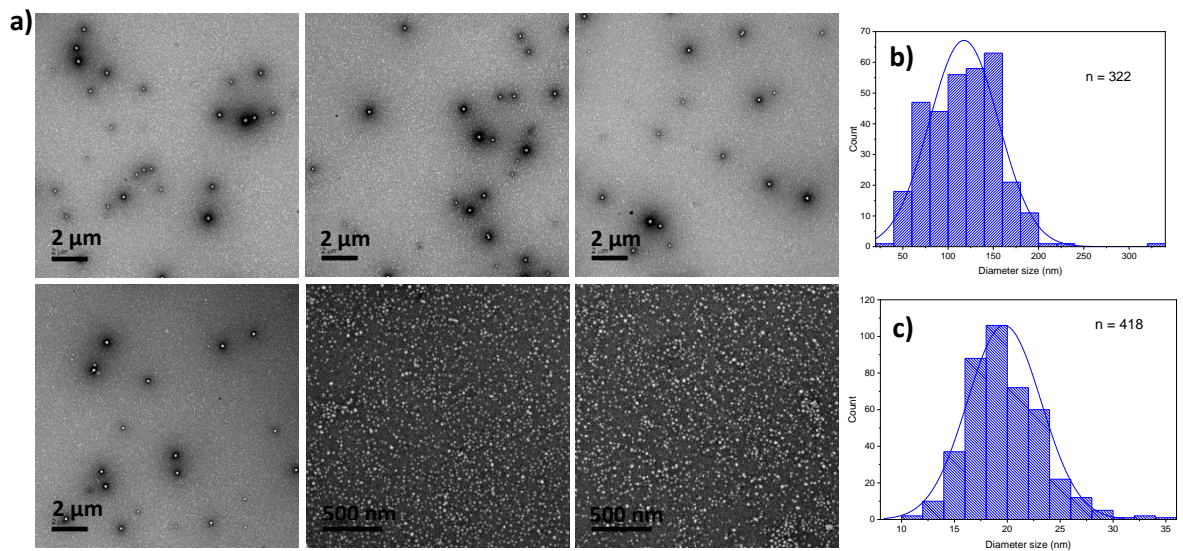


Fig. S68. a) TEM images of **poly5b-b-poly10b [50:50]** self-assembled in acetone; b) distribution of bigger particles with average size (118 ± 38) nm; c) distribution of smaller particles with average size (20 ± 3) nm.

6.3. Poly4-b-poly2 [50:50] in tetrahydrofuran

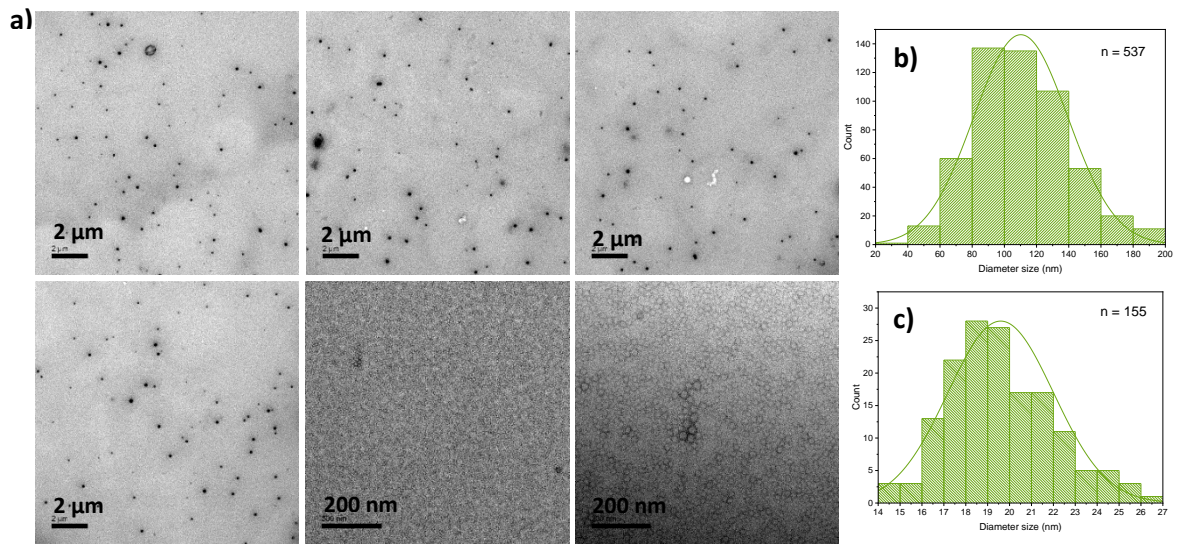


Fig. S69. a) TEM images of **poly5b-b-poly10b [50:50]** self-assembled in THF; b) distribution of bigger particles with average size (110 ± 29) nm; c) distribution of smaller particles with average size (20 ± 2) nm.

6.4. Poly4-b-poly2 [64:36] in acetone

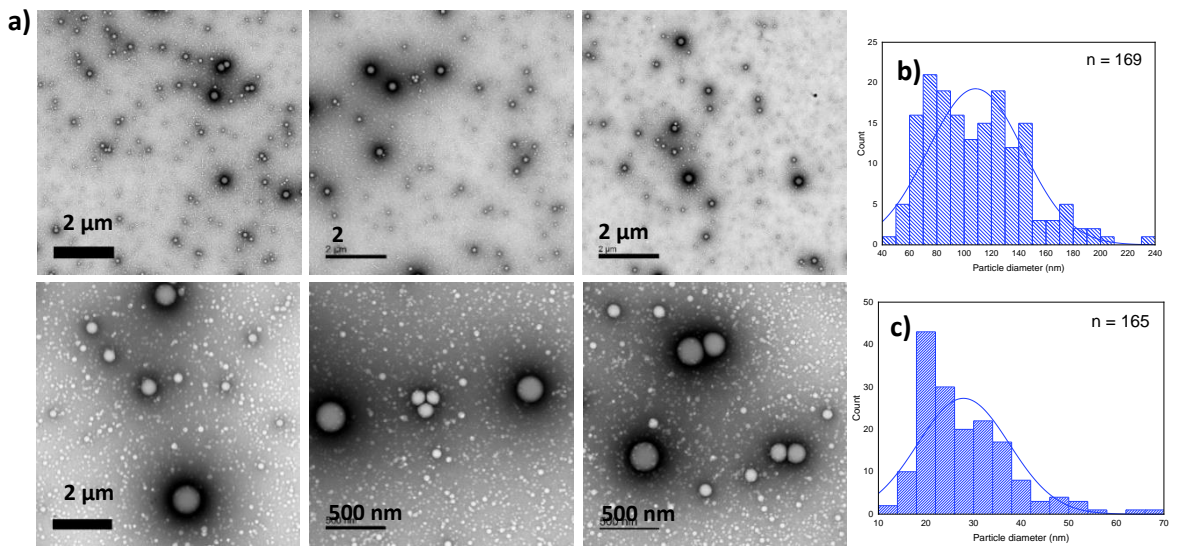


Fig. S70. a) TEM images of **poly5b-b-poly10b [64:36]** self-assembled in acetone; b) distribution of bigger particles with average size (108 ± 35) nm; c) distribution of smaller particles with average size (28 ± 9) nm.

6.5. Poly4-co-poly2 [60:40] in acetone

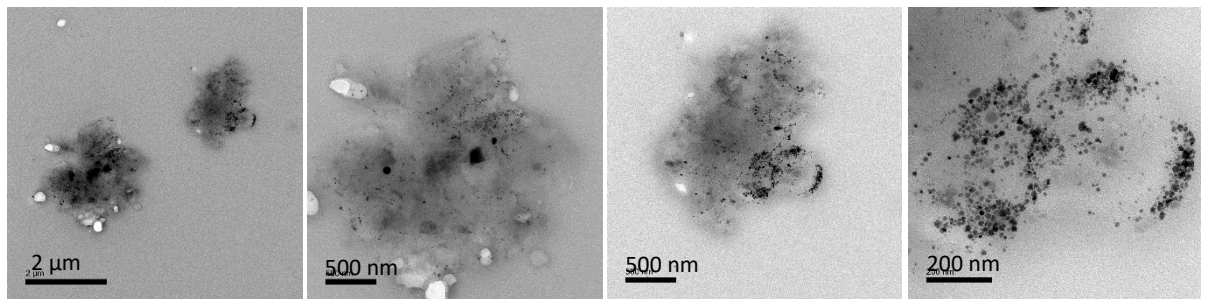


Fig. S71. TEM images of **poly5b-co-poly10b [60:40]** self-assembled in acetone.

6.6. Poly4-co-poly2 [60:40] in tetrahydrofuran

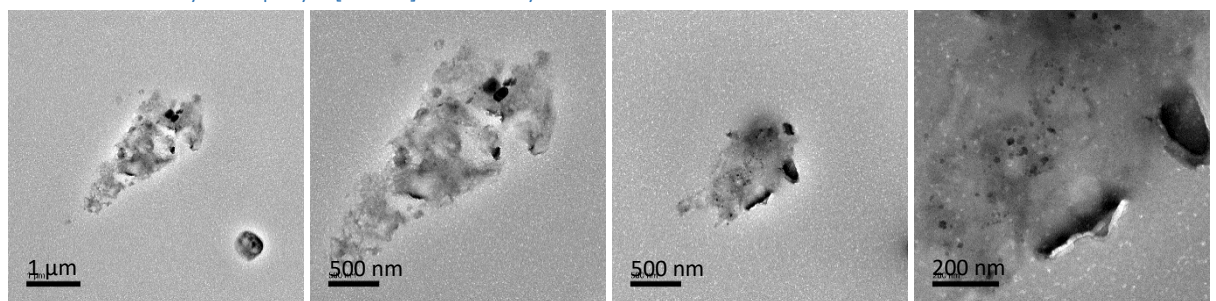


Fig. S72. TEM images of **poly5b-co-poly10b [60:40]** self-assembled in THF.

6.7. Poly4-co-poly2 [60:40] in acetonitrile

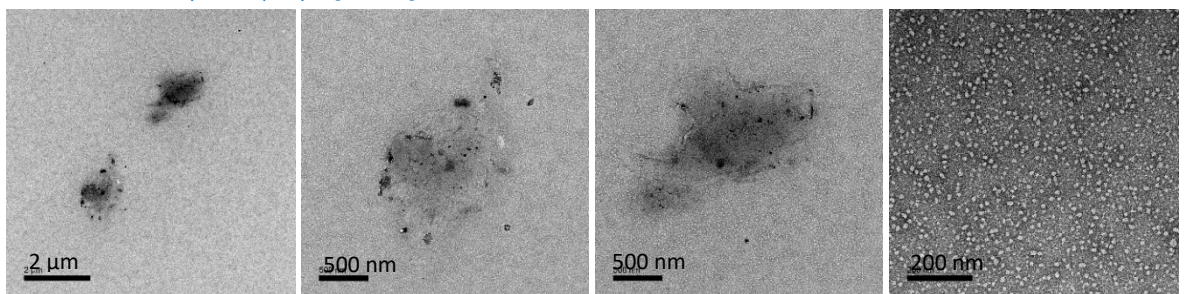


Fig. S73. TEM images of poly5b-co-poly10b [60:40] self-assembly in acetonitrile.

6.8. Poly4-co-poly2 [63:37] in acetone

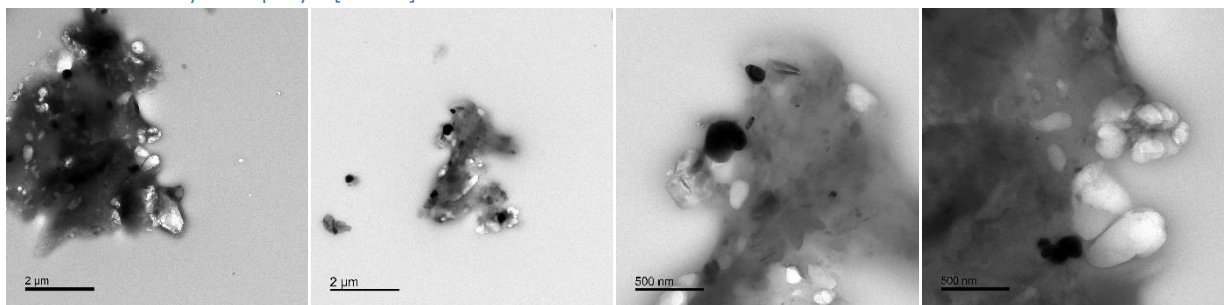


Fig. S74. TEM images of poly5b-co-poly10b [63:37] self-assembled in acetone.

7. *In vitro* release studies from polymeric nanoparticles

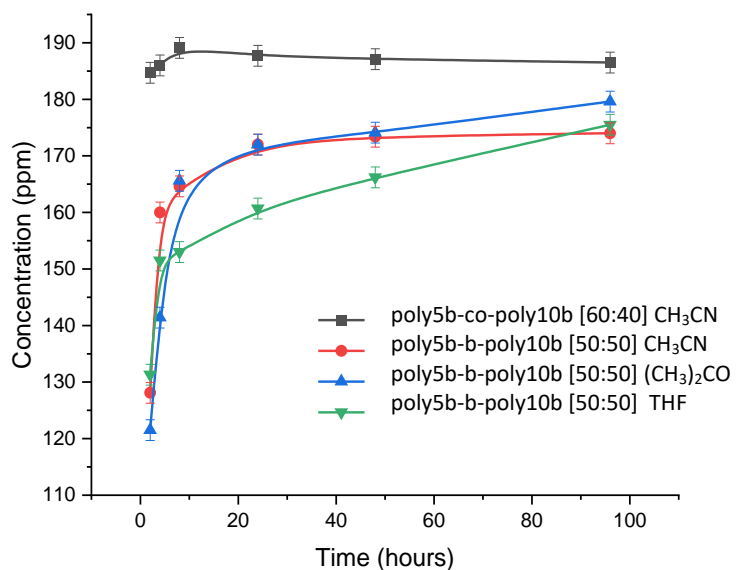


Fig. S75. Graph concentration of ibuprofen released over time in 2M NaOH. Nanoparticles have been obtained by dissolving the polymer (**poly5b-b-poly10b [50:50]** and **poly5b-co-poly10b [60:40]**) in different organic solvents such as acetonitrile, acetone and THF and then by nanoprecipitation with deionised water.

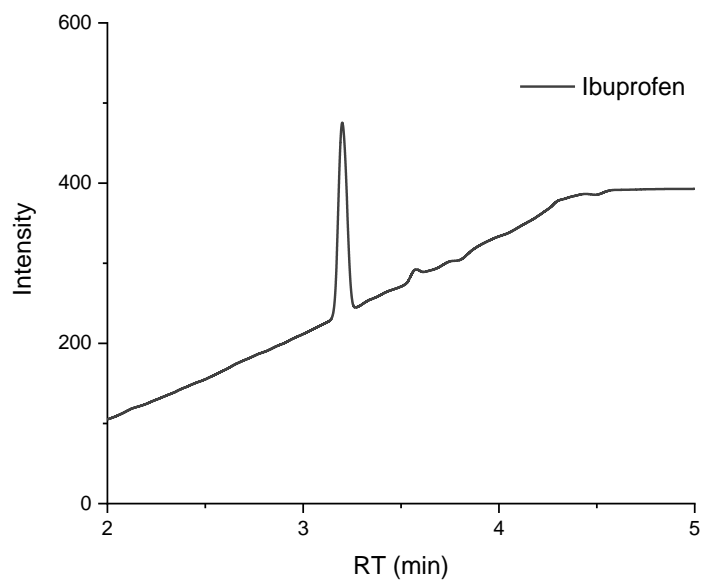


Fig. S76. Chromatogram showing that the ibuprofen detected after hydrolysis possesses a retention time of 3.2 minutes

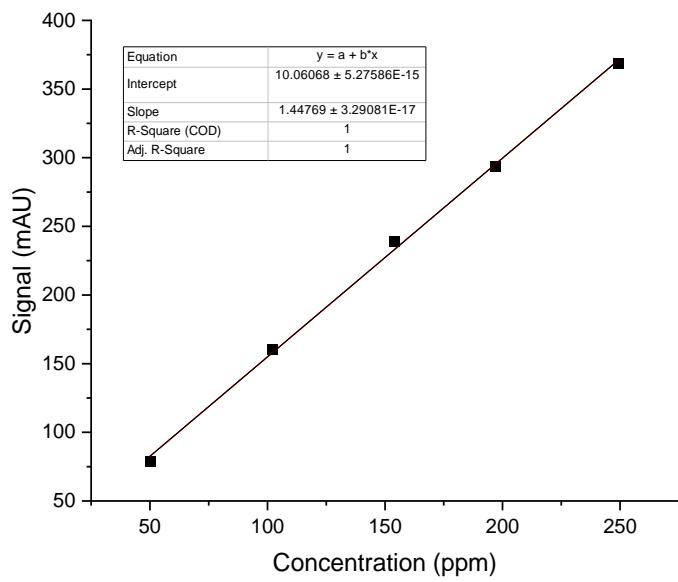


Fig. S77. HPLC calibration curve. Standards of ibuprofen in methanol at 50, 100, 150, 200 and 250 ppm were prepared and analysed by HPLC.

8. References

- 1 Y. C. Teo and Y. Xia, *Macromolecules*, 2015, **48**, 5656–5662.
- 2 S. C. G. Biagini and A. L. Parry, *J. Polym. Sci. Part A Polym. Chem.*, 2007, **45**, 3178–3190.
- 3 S. C. G. Biagini, S. M. Bush, V. C. Gibson, L. Mazzariol, M. North, W. G. Teasdale, C. M. Williams, G. Zagotto and D. Zamuner, *Tetrahedron*, 1995, **51**, 7247–7262.